Overview of Arraying Techniques in the Deep Space Network

A. Mileant
Telecommunications Systems Section

S. Hinedi
Communications Systems Research Section

Four different arraying schemes that can be employed by the Deep Space Network are functionally discussed and compared. These include symbol stream combining (SSC), baseband combining (BC), carrier arraying (CA), and full spectrum combining (FSC). In addition, sideband aiding (SA) is also included and compared even though it is not an arraying scheme, since it employs a single antenna. Moreover, combinations of these schemes are discussed, such as carrier arraying with sideband aiding and baseband combining (CA/SA/BC) or carrier arraying with symbol stream combining (CA/SSC). Complexity versus performance is traded off throughout the article and the benefits to the reception of existing spacecraft signals are discussed. Recommendations are made as to the best techniques for particular configurations.

I. Introduction

As the signal arriving from a receding deep-space spacecraft becomes weaker and weaker each year, the need arises to devise schemes to compensate for the reduction in signal-to-noise ratio (SNR). With maximum antenna apertures and lower noise temperatures pushed to their limits, the only remaining method to improve the effective SNR is to "combine" the signals from several antennas. This is referred to as arraying and it enables the Deep Space Network (DSN) to extend the missions of spacecraft beyond their planned duration. Another advantage of arraying is its ability to receive higher data rates than can be supported with a single existing antenna. As an example, symbol stream combining was used to array symbols between the Very Large Array (VLA) radio telescope and Goldstone's antennas during Voyager's encounter at Neptune [1,2]. That technique increased the scientific return from the spacecraft by allowing data transmission at a higher rate. In general, arraying enables a communication link to operate with, effectively, a larger antenna than is physically available.

There are various arraying techniques that have been considered and analyzed in the past. The purpose of this article is to functionally unify and compare the various algorithms and techniques by pointing out their relative ad-

vantages and disadvantages. Antenna arraying can be employed with any signal modulation format: bi-phase shift keyed (BPSK), quadrature phase shift keyed (QPSK), continuous phase modulation (CPM), etc. In this article, the National Aeronautics and Space Administration (NASA) standard deep-space signal format is used to illustrate the different arraying techniques, but the results can be extended to other formats, including suppressed carriers.

It is well known [3] that the received signals from deep-space spacecraft take on the following format:

$$r(t) = \sqrt{2P}\sin[\omega_c t + \Delta d(t)\,\text{sq}(\omega_{sc}t + \theta_{sc}) + \theta_c] + n(t) \quad (1)$$

where $n(t)$ is an additive bandlimited white Gaussian noise process, P is the total received signal power, ω_c and θ_c are the carrier frequency and phase, respectively, Δ is the modulation index, $d(t)$ is the nonreturn-to-zero or Manchester data, and $\text{sq}(\omega_{sc}t + \theta_{sc})$ is the square-wave subcarrier with frequency ω_{sc} and phase θ_{sc}. The received signal can be rewritten alternatively as

$$r(t) = \sqrt{2P_C}\sin(\omega_c + \theta_c) + \sqrt{2P_D}\,d(t)\,\text{sq}(\omega_{sc}t + \theta_{sc}) \times \cos(\omega_c + \theta_c) + n(t) \quad (2)$$

where P_C and P_D are the carrier and data powers and are given by $P\cos^2\Delta$ and $P\sin^2\Delta$, respectively. The first component is the residual carrier, typically tracked by a phase-locked loop, and the second component is the suppressed carrier which can be tracked by a Costas loop. The modulation $d(t)$ is given by

$$d(t) = \sum_{k=-\infty}^{\infty} d_k p(t - kT_s) \quad (3)$$

where d_k is the ± 1 binary data and T_s is the symbol period. The primary function of a receiver is to coherently detect the transmitted symbols as illustrated in Fig. 1. The demodulation process requires carrier, subcarrier, and symbol synchronization. Ideally, the output of the receiver x_k is given by

$$x_{k,ideal} = \sqrt{P_D}\,d_k + n_k \quad (4)$$

where n_k is a Gaussian random variable. In the sections to follow, performance of a particular arraying scheme is measured in terms of its degradation with respect to the ideal gain that can be attained, which assumes no combining or synchronization losses. In the simplest case, using two identical antennas with two separate but identical receivers to demodulate the received signal, ideally the output of each receiver would be similar to Eq. (4) and the noise samples of each stream would be independent. Therefore, if the symbol streams were properly aligned and added, the symbol SNR of the combined symbol stream would be 3 dB higher than the symbol SNR of the individual streams, resulting in an ideal 3-dB gain.

Typically, however, the carrier, subcarrier, and symbol synchronizations result in signal degradation and the output of the receiver is more realistically modeled by [3]:

$$x_k = \sqrt{P_D}\,d_k\cos\phi_c\left(1 - \frac{2}{\pi}|\phi_{sc}|\right)\left(1 - \frac{1}{2\pi}|\phi_{sy}|\right) + n_k \quad (5)$$

where ϕ_c, ϕ_{sc}, and ϕ_{sy} denote carrier, subcarrier, and symbol phase errors, respectively. It is worth noting at this point the difference between symbol SNR degradation and symbol SNR loss. Symbol SNR degradation is defined as the average reduction in SNR at the symbol matched filter output due to imperfect carrier, subcarrier, or symbol synchronization. For example, the SNR degradation due to imperfect carrier reference is given by

$$\overline{C_c^2} = \overline{\cos^2\phi_c} \quad (6)$$

where the overbar denotes expectation with respect to the carrier phase error ϕ_c. Symbol SNR loss, on the other hand, is defined as the additional symbol SNR needed in the presence of imperfect synchronization to achieve the same symbol error probability as in the presence of perfect synchronization. The latter is typically larger than the SNR degradation, but both degradation and loss are comparable at high loop SNRs [3]. For the purpose of comparing arraying schemes, this article considers symbol SNR degradation, which is easier to compute and is more or less indicative of the error probability performance in the region of interest. In order to simplify this notation, rewrite Eq. (5) as follows:

$$x_k = \sqrt{P_D}\,C_c C_{sc} C_{sy} d_k + n_k \quad (7)$$

where C_c, C_{sc}, and C_{sy} denote the carrier, subcarrier, and symbol "reduction" functions and are given by $C_c = \cos\phi_c$, $C_{sc} = 1 - (2/\pi)|\phi_{sc}|$, and $C_{sy} = 1 - (1/2\pi)|\phi_{sy}|$, respectively. Sometimes it is convenient to use C_t to denote the total degradation given by

$$C_t = C_c C_{sc} C_{sy} \quad (8)$$

There are basically four different arraying schemes that can be employed by the DSN. These are symbol stream combining (SSC), baseband combining (BC), carrier arraying (CA), and full spectrum combining (FSC). In addition, sideband aiding (SA) can also be employed, even

though it is not an arraying technique as it employs a single antenna. The next sections will functionally discuss these various schemes and try to clarify their advantages. Furthermore, a combination of these schemes will be discussed, such as carrier arraying with sideband aiding and baseband combining (CA/SA/BC) or carrier arraying with symbol stream combining (CA/SSC), just to name a few. Complexity versus performance will be traded off throughout the article and benefits to the reception of existing spacecraft signals are discussed.

II. Symbol SNR Degradation Due to Imperfect Synchronization

Before proceeding with arraying, it is crucial to understand and quantify the individual degradations due to the carrier, subcarrier, and symbol synchronizations to assess which of these is the dominant term and how each can be reduced. The results that follow are well known and will be used in subsequent sections to compare arraying schemes.

In the Advanced Receiver II (ARX II) [4], carrier tracking can be performed in two ways. The residual component of the signal can be tracked with a phase-locked loop (PLL) or the suppressed component of the signal can be tracked with a Costas loop. With a PLL, the loop SNR is given by

$$\rho_{c,r} \triangleq \frac{1}{\sigma_{c,r}^2} = \frac{P_C}{N_0 B_c} \tag{9}$$

where B_c is the carrier loop bandwidth and $\sigma_{c,r}^2$ is the phase jitter in the loop (the subscript c,r refers to the carrier residual component). On the other hand, with a Costas loop,

$$\rho_{c,s} \triangleq \frac{1}{\sigma_{c,s}^2} = \frac{P_D S_L}{N_0 B_c} \tag{10}$$

where S_L is the squaring loss given by

$$S_L = \frac{1}{1 + [1/(2E_s/N_0)]} \tag{11}$$

and $E_S/N_0 = P_D T_s/N_0$ is the symbol SNR (the subscript c,s refers to the carrier suppressed component). Note from Eq. (2) that when $\Delta = 90$ deg, the residual component disappears and the carrier is fully suppressed. On the other hand, when $\Delta = 0$ deg, the signal reduces to a pure sine wave. Typically both components of the carrier, residual and suppressed, can be tracked simultaneously and the carrier phase estimates combined to provide an improved estimate. This is referred to as sideband aiding and it results in an improved loop SNR given to a first-order approximation [5] by

$$\rho_c = \rho_{c,r} + \rho_{c,s} \tag{12}$$

Whether sideband aiding is employed or not, the degradation due to imperfect carrier reference is still given by $\overline{C_c^2}$. Assuming a carrier phase error density function of the form [6]:

$$p(\phi_c) = \frac{e^{\rho_c \cos\phi_c}}{2\pi I_0(\rho_c)} \tag{13}$$

the carrier degradation, $\overline{C_c^2}$, becomes

$$\overline{C_c^2} = \frac{1}{2}\left[1 + \frac{I_2(\rho_c)}{I_0(\rho_c)}\right] \tag{14}$$

where $I_k(x)$ denotes the modified Bessel function of order k. Note that the Tikhonov density of Eq. (13) is valid only in the case of a first-order PLL. It will, however, be used as an approximation for other synchronization loops, including the subcarrier and the symbol loops, with the carrier loop SNR replaced by the SNR of the respective loop. The degradation $\overline{C_c^2}$ is shown in Fig. 2 as a function of the ratio of the total received signal power to the one-sided noise spectral level (i.e., P_T/N_0), in the presence and absence of sideband aiding. From the figure, it is clear that sideband aiding can reduce the carrier degradation significantly when the data power is sufficiently "large," i.e., when the modulation index is relatively "high." Furthermore, an "x" has been placed in the figure indicating the point where the carrier loop SNR drops below 8 dB and significant cycle slipping occurs. From Fig. 2, the loop maintains lock at 22.5 dB-Hz with SA, but requires at least 27.5 dB-Hz without sideband aiding, resulting in a 5-dB higher operating threshold.

Another useful quantity is the average amplitude degradation due to imperfect carrier synchronization, given by

$$\overline{C_c} = \frac{I_1(\rho_c)}{I_0(\rho_c)} \tag{15}$$

It will be used in subsequent sections to compute the SNR degradation of various arraying schemes. As for the subcarrier and symbol phase errors, consider two cases, one where the densities are assumed Gaussian, and the other where they are approximated by the Tikhonov density of Eq. (13). Both approximations are expected to agree at high loop SNRs, but not necessarily at low loop SNRs. The exact densities of the phase errors are not known and remain an open problem. For either density,

$$\overline{C_{sc}} = 1 - \frac{2}{\pi}\overline{|\phi_{sc}|} \tag{16}$$

$$\overline{C_{sy}} = 1 - \frac{1}{2\pi}\overline{|\phi_{sy}|} \tag{17}$$

$$\overline{C_{sc}^2} = 1 - \frac{4}{\pi}\overline{|\phi_{sc}|} + \frac{4}{\pi^2}\overline{\phi_{sc}^2} \tag{18}$$

$$\overline{C_{sy}^2} = 1 - \frac{1}{\pi}\overline{|\phi_{sy}|} + \frac{1}{4\pi^2}\overline{\phi_{sy}^2} \tag{19}$$

where

$$\overline{|\phi|} = \sqrt{\frac{2}{\pi}}\sigma \tag{20}$$

$$\overline{\phi^2} = \sigma^2 \tag{21}$$

for the Gaussian densities, and σ^2 denotes the variance of the phase error, i.e., $\rho = 1/\sigma^2$. Now, let ρ denote the loop SNR, then

$$\overline{|\phi|} = \frac{1}{\pi I_0(\rho)} \sum_{k=0}^{\infty} \epsilon_k I_k(\rho) \frac{1}{k^2}[(-1)^k - 1] \tag{22}$$

$$\overline{\phi^2} = \frac{2}{I_0(\rho)} \sum_{k=0}^{\infty} \epsilon_k I_k(\rho) \frac{(-1)^k}{k^2} \tag{23}$$

for the Tikhonov densities ($\epsilon_0 = 1$ and $\epsilon_k = 2$ for $k \neq 0$). The subcarrier loop phase jitter, σ_{sc}^2, in a Costas loop is given by (W_{sc} denotes the subcarrier window) [7]:

$$\sigma_{sc}^2 = \frac{1}{\rho_{sc}} = \left(\frac{\pi}{2}\right)^2 \frac{B_{sc}W_{sc}}{R_s(E_s/N_0)}\left(1 + \frac{E_s}{N_0}\right) \tag{24}$$

Similarly, the symbol loop phase jitter, σ_{sy}^2, assuming a data transition tracking loop, is [6]:

$$\sigma_{sy}^2 = \frac{1}{\rho_{sy}} = 2\pi^2 \frac{B_{sy}W_{sy}}{R_s(E_s/N_0)\,\mathrm{erf}^2(\sqrt{E_s/N_0})} \tag{25}$$

where W_{sy} is the symbol window, $R_s = 1/T_s$ is the symbol rate, and $\mathrm{erf}(x)$ denotes the error function. The subcarrier and symbol degradations, $\overline{C_{sc}^2}$ and $\overline{C_{sy}^2}$, are depicted in Fig. 3 versus the loop SNR for both approximations.

Typically, the DSN operates with a subhertz loop bandwidth for the subcarrier and symbol synchronization loops, resulting in negligible degradation from imperfect subcarrier and symbol phase references. In most situations, the carrier degradation is the dominant term and can be as large as 0.8 dB for very weak signals, with an 8-dB loop SNR. Since both approximations yield similar degradations, the performances of the various schemes in the subsequent sections are derived using the Gaussian model for the phase errors.

III. Arraying Techniques

As mentioned previously, a 3-dB improvement in symbol SNR is expected, assuming an array of two identical antennas with ideal synchronization. In this section, the effective symbol SNR is derived for the various arraying schemes, assuming L antennas and accounting for imperfect synchronization. Moreover, included here is the effect of sideband aiding and a comparison of performance versus complexity for all schemes.

A. Symbol Stream Combining (SSC)

Symbol stream combining is depicted in Fig. 4. Each antenna tracks the carrier and the subcarrier and performs symbol synchronization individually. The symbols at the output of each receiver are then combined, with the appropriate weights, to form the final detected symbols. The advantage of SSC is that the combining loss is negligible [8] and is performed in the data rate bandwidth. Moreover, antennas that are continents apart can transmit their symbols in real or non-real time to a central location where the symbol stream combiner outputs the final symbols. That, however, requires that each antenna be able to lock on the signal individually. The disadvantage of SSC is that L carrier, L subcarrier, and L symbol tracking devices are needed, and each suffers some degradation. For "moderate" to "high" modulation indices, the carrier degradation can be reduced by employing sideband aiding at each antenna. The samples of the signal at the output of the symbol stream combiner are

$$v_k = d_k \sum_{i=1}^{L} \beta_i \sqrt{P_{Di}} \cos\phi_{ci}\left(1 - \frac{2}{\pi}|\phi_{sci}|\right) \times \left(1 - \frac{1}{2\pi}|\phi_{syi}|\right) + n_k' \tag{26}$$

where β_i's are weighing factors, $P_{Di} = P_i \sin^2\Delta$ is the received data power at antenna i (P_i is total received power), and ϕ_{ci}, ϕ_{sci}, and ϕ_{syi} are the carrier, subcarrier, and symbol phase errors, respectively, at the ith antenna. There is negligible loss when combining the symbols (< 0.05 dB)

and, assuming that each receiver chain has a one-sided noise power spectral density level N_{0i}, it is straightforward to show [9] that the variance of n'_k is given by

$$\sigma^2_{n'} = \frac{1}{2T_s} \sum_{i=1}^{L} \beta_i^2 N_{0i} \tag{27}$$

The conditional symbol SNR (assuming that the various phase errors are known) at the output of the combiner is defined as

$$SNR' = \frac{(\overline{v_k})^2}{\sigma^2_{n'}} \tag{28}$$

where $\overline{v_k}$ is the conditional mean of v_k. Using Eq. (27),

$$SNR' = \frac{2P_{D1}T_s}{N_{01}} \frac{\left(\sum_{i=1}^{L} \beta_i \sqrt{P_{Di}/P_{D1}} C_{ti} \right)^2}{\sum_{i=1}^{L} \beta_i^2 (N_{0i}/N_{01})} \tag{29}$$

where C_{ti} is defined in Eq. (8). Letting $\beta_1 = 1$ and optimizing β_i's ($i = 2, \ldots, L$) in order to maximize SNR', one obtains

$$\beta_i = \sqrt{\frac{P_i}{P_1}} \frac{N_{01}}{N_{0i}} \tag{30}$$

Plugging back in Eq. (29), one gets

$$SNR' = \frac{2P_{D1}T_s}{N_{01}} \frac{\left(\sum_{i=1}^{L} \gamma_i C_{ti} \right)^2}{\sum_{i=1}^{L} \gamma_i} \tag{31}$$

where γ_i is defined as

$$\gamma_i = \frac{P_i}{P_1} \frac{N_{01}}{N_{0i}} \tag{32}$$

where

$$\Gamma \triangleq \sum_{i=1}^{L} \gamma_i$$

The γ_i factors for various DSN antennas are given in Appendix A for both S-band (2.2 to 2.3 GHz) and X-band (8.4 to 8.5 GHz). Note that in the absence of any degradation ($C_{ti} = 1$ for $i = 1, \ldots, L$), the conditional SNR simplifies to

$$SNR_{ideal} = \frac{2P_{D1}T_s}{N_{01}} \sum_{i=1}^{L} \gamma_i = \frac{2P_{D1}T_s}{N_{01}} \Gamma \tag{33}$$

with Γ being the "ideal gain factor" obtained at antenna 1, which will be denoted the master antenna for pure convenience (when $\gamma_i = \gamma_1$ for all i, $\Gamma = L$). For two identical antennas with equal noise temperatures, $\gamma_1 = \gamma_2 = 1$ and the conditional SNR reduces to $4P_{D1}T_s/N_{01}$ as expected, i.e., an effective gain of 3 dB. The unconditional SNR at the output of the symbol combiner is obtained by averaging the conditional SNR over the unknown phase errors, which are embedded in the constant C_{ti}'s, i.e.,

$$SNR = \frac{2P_{D1}T_s}{N_{01}} \left(\frac{\sum_{i=1}^{L} \gamma_i^2 \overline{C_{ti}^2} + \sum \sum_{\substack{i,j \\ i \neq j}} \gamma_i \gamma_j \overline{C_{ti}}\, \overline{C_{tj}}}{\Gamma} \right) \tag{34}$$

where

$$\overline{C_{ti}^2} = \overline{C_{ci}^2}\, \overline{C_{sci}^2}\, \overline{C_{syi}^2} \quad \text{and} \quad \overline{C_{ti}} = \overline{C_{ci}}\, \overline{C_{sci}}\, \overline{C_{syi}} \tag{35}$$

Because the noise processes make all the phase errors mutually independent, the computation of the unconditional SNR in Eq. (34) reduces to the computation of the first two moments of the various values of C_{ci}, C_{sci}, and C_{syi}. Finally, the SNR "degradation factor" D_{ssc} (in decibels) for symbol stream combining is defined as

$$D_{ssc} = 10 \log_{10} \left(\frac{SNR}{SNR_{ideal}} \right)$$

$$= 10 \log_{10} \left(\frac{\sum_{i=1}^{L} \gamma_i^2 \overline{C_{ti}^2} + \sum \sum_{\substack{i,j \\ i \neq j}} \gamma_i \gamma_j \overline{C_{ti}}\, \overline{C_{tj}}}{\Gamma^2} \right) \tag{36}$$

Note that D_{ssc} is a negative number that ideally approaches zero. In general, the larger the D_{ssc}, the better the symbol stream combining performance. For the case of a single antenna (i.e., no arraying), D_{ssc} measures the degradation due to imperfect synchronization. Figure 5 depicts D_{ssc} for the array of two high-efficiency (HEF) and one standard (STD) 34-m antennas as a function of P_T/N_0 of the master antenna, Fig. 5(a), and modulation index, Fig. 5(b). In this case, the ideal expected gain is 2.6 dB, but only a fraction of that is attained, depending on the received P_T/N_0 and Δ. The figures also depict the corresponding carrier, subcarrier, and symbol degradations and it is clear that the carrier provides the dominant term.

B. Baseband Combining (BC)

In baseband combining, each antenna locks on the signal by itself as depicted in Fig. 6. The baseband signals, consisting of data on a subcarrier, are then combined and the symbols demodulated. The combining is performed by the baseband assembly (BBA), which consists of three elements: the real-time combiner (RTC), the subcarrier loop, and the symbol tracking loop. The inputs to the BBA are analog baseband telemetry signals from L receivers ($L \leq 8$) and the output is a sequence of combined digital symbols given by

$$v_k = d_k\left(1 - \frac{2}{\pi} \mid \phi_{sc} \mid\right)\left(1 - \frac{1}{2\pi} \mid \phi_{sy} \mid\right) \times \sum_{i=1}^{L} \beta_i \sqrt{P_{Di}} \cos\phi_{ci}(1 - 4m \mid \tau_i \mid) + n'_k \quad (37)$$

where m is the ratio of the subcarrier frequency over the symbol rate and τ_i is the delay error of the ith RTC loop ($\tau_1 \equiv 0$) [10]. Since the BBA employs baseband combining (i.e., combines the signals prior to the subcarrier loop), only one subcarrier and one symbol tracking loop are employed and no subscripts are needed for the random variables ϕ_{sc} and ϕ_{sy}. The variance of v_k due to thermal noise is still given by Eq. (27). Again, as with the SSC scheme, the conditional SNR at the output of the symbol tracking loop is given by

$$SNR' \triangleq \frac{(\overline{v_k})^2}{\sigma^2_{n'}} = \frac{2P_{D1}T_s}{N_{01}} \frac{\left(C_{sc}C_{sy}\sum_{i=1}^{L}\beta_i\sqrt{P_{Di}/P_{D1}}C_i\right)^2}{\Gamma} \quad (38)$$

where the SNR degradation function C_i accounts for the carrier and delay degradations and is defined as

$$C_i = C_{ci}C_{\tau i} = \cos\phi_{ci}(1 - 4m \mid \tau_i \mid) \quad (39)$$

In order to compute the unconditional SNR at the output of the symbol tracking loop, Eq. (38) is averaged over all the phase and delay error processes in the corresponding tracking loops, resulting in

$$SNR = \frac{2P_{D1}T_s}{N_{01}} \overline{C^2_{sc}}\;\overline{C^2_{sy}} \left(\frac{\sum_{i=1}^{L}\gamma_i^2\overline{C_i^2} + \sum\sum_{\substack{i,j \\ i\neq j}}\gamma_i\gamma_j\overline{C_i}\;\overline{C_j}}{\Gamma}\right) \quad (40)$$

The signal reduction function for the RTC, denoted by $C_{\tau i}$ and given by $(1 - 4m \mid \tau_i \mid)$, has the following first two moments:

$$\overline{C_{\tau i}} = \left(1 - 4m\sqrt{\frac{2}{\pi}}\sigma_{\tau i}\right) \quad (41a)$$

and

$$\overline{C^2_{\tau i}} = \left(1 - 8m\sqrt{\frac{2}{\pi}}\sigma_{\tau i} + 16m^2\sigma^2_{\tau i}\right) \quad (41b)$$

where $\sigma^2_{\tau i}$ denotes the variance of the ith loop of the real-time combiner and is computed to be [10]:

$$\sigma^2_{\tau i} = \frac{B_{\tau i}}{B_n 32m^2} \times \left\{\frac{1}{\left[\mathrm{erf}\left(\sqrt{P_{D1}\sigma_1^2}\right)\mathrm{erf}\left(\sqrt{P_{Di}\sigma_i^2}\right)\right]^2} - 1\right\} \quad (42)$$

In the above equation, $i = 2, \ldots, L$, $B_{\tau i}$ denotes the bandwidth of the RTC loops, B_n denotes the noise bandwidth at the RTC input (assumed the same in all channels), and $\sigma_i^2 = N_{0i}B_n$ (note that $\overline{C_{\tau 1}} \equiv 1$ and $\overline{C^2_{\tau 1}} \equiv 1$).

The equations for the moments of C_{sc} and C_{sy} are those given by Eqs. (16) through (19), with the variances computed using the combined P_D/N_0. Note that under ideal conditions (i.e., no phase or delay errors in the tracking loops), all C's are 1 and the SNR reduces to

$$SNR_{ideal} = \frac{2P_{D1}T_s}{N_{01}}\Gamma \quad (43)$$

as in the symbol stream combining case, Eq. (33). As expected, both SSC and BC have the same SNR performance under ideal conditions. Once the unconditional SNR is computed for the BC scheme using Eq. (40), the degradation factor is obtained as before, namely,

$$D_{bc} = 10\log_{10}\left(\frac{SNR}{SNR_{ideal}}\right) = 10\log_{10}\left(\overline{C^2_{sc}}\;\overline{C^2_{sy}}\,\frac{\sum_{i=1}^{L}\gamma_i^2\overline{C_i^2} + \sum\sum_{\substack{i,j \\ i\neq j}}\gamma_i\gamma_j\overline{C_i}\;\overline{C_j}}{\Gamma^2}\right) \quad (44)$$

Figure 7 depicts the degradation due to baseband combining, D_{bc}, as a function of both P_T/N_0, Fig. 7(a), and Δ, Fig. 7(b), assuming the same array as in the SSC case. The noise bandwidth of the RTC was set to 132 kHz to pass the fifth harmonic of the subcarrier with frequency 32.768 kHz. Note from Fig. 7(a) that the subcarrier and symbol degradations are less than their counterparts in SSC, Fig. 5(a). However, there is an additional combining loss of about 0.2 dB that is not present in the SSC.

C. Full Spectrum Combining (FSC)

Full spectrum combining is an arraying technique where the signals are combined at intermediate frequency (IF) as depicted in Fig. 8. One receiver chain, consisting of one carrier, one subcarrier, and one symbol synchronization loop, is then used to demodulate the signal. The combining at IF is two dimensional in the sense that both delay and phase adjustment are required to coherently add the signals. Let the received signal at antenna 1 be denoted by $s_1(t)$. Then from Eq. (1),

$$s_1(t) = \sqrt{2P_1}\sin[\omega_c t - \theta_1(t)] \tag{45}$$

where $\theta_1(t) = \theta_M(t)+\theta_D(t)+\theta_{osc}(t)$, $\theta_M(t)$ represents the biphase modulation, $\theta_D(t)$ is the Doppler due to spacecraft dynamics, and $\theta_{osc}(t)$ is the oscillator phase noise.

The received signals at the other antennas are delayed versions of $s_1(t)$ and are given by

$$s_i(t) = s(t-\tau_i) = \sqrt{2P_i}\sin[\omega_c(t-\tau_i)+\theta_i(t-\tau_i)] \tag{46}$$

for $i = 2, \ldots L$, where τ_i denotes the delay in signal reception between the first and the ith antennas ($\tau_1 \equiv 0$), and $\theta_i(t) = \theta_1(t) + \Delta\theta_i(t)$. In this case, $\Delta\theta_i(t)$ accounts for differential Doppler and phase noises, which are typically "very small." Note that at the RF frequency ω_c, the signal $s_i(t)$ can be delayed by $-\tau_i$ and added coherently, as long as the τ_i's are known. So combining can be achieved at RF with only a delay adjustment. Downconverting the delayed signals to IF (ω_I denotes the IF frequency) yields

$$y_i(t) = \sqrt{2P_i}\sin[\omega_I t - \omega_c\tau_i + \theta_i(t-\tau_i)] \tag{47}$$

and delaying each signal $y_i(t)$ by $-\tau_i$, gives

$$\begin{aligned} z_i(t) &= y_i(t+\tau_i) \\ &= \sqrt{2P_i}\sin[\omega_I t - \omega_c\tau_i + \omega_I\tau_i + \theta_1(t) + \Delta\theta_i(t)] \end{aligned} \tag{48}$$

for $i \neq 1$. The signal's $z_i(t)$'s cannot be added coherently because the phases are not aligned, due to the factor $(\omega_I - \omega_c)\tau_i$, even though the data are aligned ($\theta_D(t)$ is part of $\theta_1(t)$). Therefore, an additional phase adjustment is necessary to add the signals coherently. This example illustrates that both delay and phase adjustments are required to add the signals coherently at IF, but that only a delay compensation is sufficient at RF. For the purpose of this article, a delay by $-\tau$ (actually, an advancement) is used for mathematical convenience. In reality, the "furthest" antenna can be used as a reference and signals from all other antennas can be delayed accordingly.

Now consider an antenna interferometric pair as illustrated in Fig. 9. The signal at antenna i arrives τ_i sec later than the signal at antenna 1, which will be used as a reference for mathematical convenience. After low noise amplification, the signals are downconverted to IF, where the ith signal is delayed by $-\tau_i$ sec. The latter delay consists of two components, a fixed component and a time-varying component. The fixed component compensates for unequal waveguide lengths between the two antennas and the correlator. It is a known quantity that can be determined by measurement. The time-varying component compensates for unequal propagation length for the two received signals. This component is typically precomputed from the trajectory of the spacecraft and the physical location of the two antennas.

The relative phase difference between the signals is estimated by performing a correlation on the resulting signals, which for all practical purposes have been aligned in time. At the input to the correlator, the two signals from the first and the ith antennas are passed through filters with bandwidth B Hz and subsequently sampled at the Nyquist rate of $2B$ samples per sec. Mathematically, the sampled signals are given by

$$z_1(t_k) = \sqrt{2P_1}\sin[\omega_I t_k + \theta_1(t_k)] + n_1(t_k)$$

and

$$z_i(t_k) = \sqrt{2P_i}\sin[\omega_I t_k + (\omega_I - \omega_c)\tau_i + \theta_i(t_k)] + n_i(t_k) \tag{49}$$

where $i \neq 1$ and $n_1(t_k)$ and $n_i(t_k)$ are independent Gaussian random variables with variances $\sigma_1^2 = N_{01}B$ and $\sigma_i^2 = N_{0i}B$. It will be shown later that the parameter B is essential in determining the averaging period and, thus, the combining loss. Correlating the signals (i.e., multiplying and lowpass filtering) yields

$$I_{i1}(t_k) = \sqrt{P_1 P_i}\cos[\phi_{i1}(t_k)] + n_{I,i1}(t_k) \tag{50}$$

where $\phi_{i1} = (\omega_I - \omega_c)\tau_i + \Delta\theta_i(t_k)$ denotes the total phase difference between the signals and $n_{I,i1}$, the effective noise, is given by

$$n_{I,i1} = \sqrt{2P_i}\sin[\omega_I t_k + \phi_{i1} + \theta_i(t_k)]n_1(t_k) + \sqrt{2P_1}\sin[\omega_I t_k + \theta_1(t_k)]n_i(t_k) + n_1(t_k)n_i(t_k) \tag{51}$$

with effective variance

$$\sigma_{ei}^2 = \sigma_1^2 P_i + \sigma_i^2 P_1 + \sigma_1^2\sigma_i^2 = B(N_{01}P_i + N_{0i}P_1) + N_{01}N_{0i}B^2 \tag{52}$$

The correlation is performed in a complex manner (i.e., four real correlations) resulting in an additional signal $Q_{i1}(t_k)$ given by

$$Q_{i1}(t_k) = \sqrt{P_1 P_i}\sin[\phi_{i1}(t_k)] + n_{Q,i1}(t_k) \tag{53}$$

The noise samples $n_{I,i1}(t_k)$ and $n_{Q,i1}(t_k)$ are uncorrelated with identical variances as given by Eq. (52). The correlator output can be represented more conveniently in a complex form as

$$\mathbf{z}_{i1}(t_k) = I_{i1}(t_k) + jQ_{i1}(t_k) \tag{54}$$

Following the correlation, an averaging operation over T sec is performed to reduce the noise effect. In that period, $N = 2BT$ independent samples are used to reduce the variance by a factor of N. The SNR at the output of the accumulator, SNR_{i1}, is thus given by

$$SNR_{i1} = \frac{NP_1P_i}{\sigma_{ei}^2} = \frac{P_1}{N_{01}}\frac{2T}{[1 + 1/\gamma_i + (BN_{0i}/P_i)]} \tag{55}$$

where γ_i is as given in Eq. (32). Note that in radiometric applications [10], the SNR is defined as the ratio of the standard deviation of the signal to that of the noise, and is the square root of the SNR defined in the above equation. Assuming that the correlation bandwidth B is "very large" (in the MHz range), the signal multiplied by the noise term $(P_1\sigma_i^2 + P_i\sigma_1^2)$ can be ignored and the effective noise variance is dominated by the noise multiplied by the noise term $(\sigma_1^2\sigma_i^2)$, i.e.,

$$\sigma_{ei}^2 \simeq \sigma_1^2\sigma_i^2 \tag{56}$$

and, hence, the SNR can be well approximated by

$$SNR_{i1} \simeq \frac{P_1}{N_{01}}\frac{P_i}{N_{0i}}\frac{2T}{B} \tag{57}$$

An estimate of ϕ_{i1}, $\widehat{\phi}_{i1}$ can be obtained by computing the inverse tangent of the real and imaginary parts of $\mathbf{z}_{i1}$, i.e.,

$$\widehat{\phi}_{i1}(t_k) = \tan^{-1}\left[\frac{Q_{i1}(t_k)}{I_{i1}(t_k)}\right] \tag{58}$$

The probability density function of such an estimate is given in [11] as

$$p(\widehat{\phi}_{i1}) = \frac{1}{2\pi}e^{-SNR_{i1}/2}\left\{1 + Ge^{G^2}\sqrt{\pi}[1 + \mathrm{erf}(G)]\right\} \tag{59}$$

where $\mathrm{erf}(x)$ is the error function and

$$G = \sqrt{\frac{SNR_{i1}}{2}}\cos(\widehat{\phi}_{i1} - \phi_{i1}) \tag{60}$$

The density in Eq. (59) is plotted in Fig. 10 and its derivation assumes that the noises $n_{I,i1}$ and $n_{Q,i1}$ are Gaussian. Even though they are not Gaussian in the strict sense, a Gaussian approximation is still justified by invoking the central limit theorem due to the averaging over N samples. Figure 10 clearly indicates that a reasonably "good" phase estimate can be obtained for SNR_{i1} as low as 6 dB. At a moderately high SNR_{i1}, the distribution can be approximated by a Gaussian distribution with variance

$$\sigma_{\Delta\phi_{i1}}^2 = \frac{1}{SNR_{i1}} \tag{61}$$

An improvement in phase error estimation can be obtained by performing global phasing between L antennas, which involves $L(L-1)/2$ complex correlations as the signal from each antenna is correlated with the signal from every other antenna. In the simplest form, the signal from antenna 1 is correlated with all other signals and the phase errors are estimated. Global phasing reduces the residual phase error variance of Eq. (61) by a factor of $L - 2$ by employing least squares calculations [11] ([2] states that the actual reduction is approximately $0.5(L-2)$, which means that global phasing gives an advantage over the conventional scheme only for $L > 4$). In addition to global phasing, closed-loop techniques can be utilized to reduce the phase error as illustrated in Appendix B.

1. Combining Loss of FSC. In order to compute the combining loss of FSC, consider the IF signals after phase compensation, i.e.,

$$\mathbf{z}_i(t_k) = \sqrt{P_i} e^{j[\omega_I t_k + \theta_1(t_k) + \Delta\phi_{i1}(t_k)]}$$

$$+ \mathbf{n}_i(t_k) e^{j[\omega_I t_k + \theta_1(t_k) + \Delta\phi_{i1}(t_k)]} \quad (62)$$

where $\Delta\phi_{i1} = \widehat{\phi}_{i1} - \phi_{i1}$ refers to the residual phase error between antenna 1 and the ith signal and $\mathbf{n}_i(t_k)$ is the complex envelope of the thermal noise with two-sided noise spectral density N_{0i}. The signal combiner performs the weighted sum of $\mathbf{z}_i(t_k)$, namely,

$$\mathbf{z}(t_k) = \sum_{i=1}^{L} \beta_i \mathbf{z}_i(t_k) = \sum_{i=1}^{L} \beta_i \left\{ \sqrt{P_i} e^{j[\omega_I t_k + \theta_1(t_k) + \Delta\phi_{i1}(t_k)]} \right.$$

$$\left. + \mathbf{n}_i(t_k) e^{j[\omega_I t_k + \theta_1(t_k) + \Delta\phi_{i1}(t_k)]} \right\} \quad (63)$$

Note that the variance of the combined complex signal $\mathbf{z}(t_k)$ is

$$\sigma_{\mathbf{z}}^2 = 2B \sum_{i=1}^{L} \beta_i^2 N_{0i} \quad (64)$$

The total signal power at the output of the combiner conditioned on residual phases, $\Delta\phi_{i1}(t_k)$, is thus given by

$$P_{\mathbf{z}}' = \left[\overline{\mathbf{z}(t_k)}\right]^2 = \sum_{i=1}^{L}\sum_{j=1}^{L} \beta_i \beta_j \sqrt{P_i P_j}\, \mathbf{C}_{IF_i} \mathbf{C}_{IF_j}^*$$

$$= \sum_{i=1}^{L} \beta_i^2 P_i \mathbf{C}_{IF_i} \mathbf{C}_{IF_i}^* + \sum_{i=1}^{L}\sum_{\substack{j=1 \\ i \neq j}}^{L} \beta_i \beta_j \sqrt{P_i P_j}\, \mathbf{C}_{IF_i} \mathbf{C}_{IF_j}^* \quad (65)$$

where

$$\mathbf{C}_{IF_i} \triangleq e^{j\Delta\phi_{i1}(t_k)} \quad (66)$$

is the complex signal reduction function due to phase misalignment between the ith and first signals. Assuming that the ensemble average of the phase difference between any two antennas is independent of which antenna pair is chosen and that the residual phase of each antenna pair is Gaussian distributed with variance $\sigma_{\Delta\phi_{i1}}^2$, then it can be shown that

$$\overline{\mathbf{C}_{IF_i} \mathbf{C}_{IF_j}^*} \triangleq C_{ij} = \mathcal{E}\{e^{j[\Delta\phi_{i1}(t_k) - \Delta\phi_{j1}(t_k)]}\}$$

$$= \begin{cases} e^{-\frac{1}{2}[\sigma_{\Delta\phi_{i1}}^2 + \sigma_{\Delta\phi_{j1}}^2]} & i \neq j,\ \sigma_{\Delta\phi_{11}}^2 \equiv 0 \\ 1 & i = j \end{cases} \quad (67)$$

Performing the above averaging operation over $P_{\mathbf{z}}'$, the total signal power is obtained, namely,

$$P_{\mathbf{z}} = P_1 \left(\sum_{i=1}^{L} \gamma_i^2 + \sum_{i=1}^{L}\sum_{\substack{j=1 \\ i \neq j}}^{L} \gamma_i \gamma_j\, C_{ij} \right) \quad (68)$$

Note that in an ideal scenario (i.e., no degradation), the signal reduction functions approach 1 ($C_{ij} = 1\ \forall\ i, j$) and Eq. (68) reduces to $P_z = P_1 L^2$. Simultaneously, the noise variance of Eq. (64) becomes proportional to L and, hence, the SNR increases linearly with L as expected.

2. Telemetry Performance of FSC. With full spectrum combining, only one receiver, one subcarrier, and symbol tracking loops are required. The samples of the signal at the output of the integrate-and-dump filter can be expressed as

$$v_k = d_k \sqrt{P_D} \cos\phi_c \left(1 - \frac{2}{\pi} \mid \phi_{sc} \mid\right) \left(1 - \frac{1}{2\pi} \mid \phi_{sy} \mid\right) + n_k' \quad (69)$$

where P_D is the combined data power given by $P_z \sin^2\Delta$ and n_k' is Gaussian with variance given by Eq. (27).

Repeating now the same steps as with either BC or SSC, it can be shown that the symbol SNR in terms of $P_{D1} = P_1 \sin^2\Delta$ is given by

$$SNR = \frac{2P_{D1}T_s}{N_{01}} \overline{C_c^2}\ \overline{C_{sc}^2}\ \overline{C_{sy}^2} \left(\frac{\sum_{i=1}^{L} \gamma_i^2 + \sum\sum_{\substack{i,j \\ i \neq j}} \gamma_i \gamma_j C_{ij}}{\Gamma} \right) \quad (70)$$

where the loop losses are computed using the combined power, being carrier or data. Note that in the ideal case, Eq. (70) reduces to SNR_{ideal} of Eq. (33) as expected. The degradation factor for the full spectrum combining scheme, D_{fsc}, is given, as before, by the ratio (in decibels) of the combined symbol SNR to the ideal symbol SNR, i.e.,

$$D_{fsc} = 10\log_{10}\left(\frac{SNR}{SNR_{ideal}}\right)$$

$$= 10\log_{10}\left(\overline{C_c^2}\ \overline{C_{sc}^2}\ \overline{C_{sy}^2} \frac{\sum_{i=1}^{L} \gamma_i^2 + \sum\sum_{\substack{i,j \\ i \neq j}} \gamma_i \gamma_j C_{ij}}{\Gamma^2} \right) \quad (71)$$

As an example, let $P_i = P_1$, $N_{0i} = N_{01}$, and $\beta_i = 1$ for all antennas, then the signal and noise powers of the real process at the output of the combiner become, respectively,

$$P_z = P_1 \left[L + 2(L-1)e^{-(\sigma^2_{\Delta\phi})/2} + (L-2)(L-1)e^{-\sigma^2_{\Delta\phi}} \right]$$

$$\sigma_z^2 = BLN_{01} \tag{72}$$

and the SNR at the combiner's output becomes

$$SNR_z = \frac{P_z}{\sigma_z^2}$$

$$= \frac{P_1 \left[L + 2(L-1)e^{-(\sigma^2_{\Delta\phi})/2} + (L-2)(L-1)e^{-\sigma^2_{\Delta\phi}} \right]}{LN_{01}B} \tag{73}$$

With perfect alignment (i.e., $\sigma^2_{\Delta\phi} \rightarrow 0$), SNR_z reduces to

$$SNR_{z,ideal} = \frac{P_1 L}{N_{01} B} \tag{74}$$

as expected and, hence, the combining degradation for the FSC scheme is given by

$$D_{fsc} =$$

$$10 \log_{10} \left[\frac{L + 2(L-1)e^{-(\sigma^2_{\Delta\phi})/2} + (L-2)(L-1)e^{-\sigma^2_{\Delta\phi}}}{L^2} \right] \tag{75}$$

Figure 11 depicts the degradation of FSC, D_{fsc}, for the same three-element array, as a function of P_T/N_0 of the master antenna, Fig. 11(a), and modulation index Δ, Fig. 11(b). It is clear from Fig. 11(a) that the FSC carrier degradation is significantly reduced over those of SSC and BC. Furthermore, the subcarrier and symbol degradations are identical to those of BC and both are much smaller than the SSC degradations, as expected. The primary advantage of FSC is that the carrier loop SNR for this particular array does not decrease below 8 dB and, hence, cycle slipping is not a major issue even at $P_T/N_0 = 20$ dB-Hz, with a 3-Hz carrier loop bandwidth.

The major drawback of FSC in this example is the long integration time required to maintain a relatively small combining loss. With $B = 2 \times 135$ kHz (IF bandwidth) and $T/B = 0.0008$ sec^2, the integration time is 216 sec, which is too long for the phase of interest to remain a constant in a practical scenario. At $P_T/N_0 = 20$ dB-Hz, the SNR at the correlator output, Eq. (57), is roughly 12 dB. In order to reduce the integration length, the correlator bandwidth can be adjusted to pass only the first harmonic of the subcarrier (i.e., $B = 2 \times 33$ kHz), resulting in a shorter integration time of 53 sec (still relatively long) and a slight degradation in correlator SNR. Note that even though the correlation is performed with only the first subcarrier harmonic, the combining should be accomplished with the full data spectrum.

D. Carrier Arraying (CA)

In carrier arraying, several carrier tracking loops are coupled in order to enhance the received carrier signal-to-noise ratio and, hence, decrease the telemetry ("radio") loss due to imperfect carrier synchronization. The coupling can be performed using phase-locked loops (PLLs) for residual carriers or Costas loops for suppressed BPSK carriers. Only the PLL case is considered in this article to illustrate the idea of carrier arraying. A general block diagram is shown in Fig. 12 where two carrier loops share information to jointly improve their performance as opposed to tracking individually. Carrier arraying by itself does not combine the data and, thus, needs to operate with baseband combining or symbol stream combining to array the telemetry. This is shown in Fig. 13 where baseband combining is employed to array the data spectra.

There are basically two scenarios where one would employ carrier arraying. In the first scenario, a "large" antenna locks on the signal by itself and then helps a "smaller" antenna track. In this case, the signal might experience dynamics requiring a large loop bandwidth and, hence, the signal has to be strong enough to enable the carrier loop to operate with the large bandwidth. A large antenna with a strong signal is first used to track the signal and then the dynamics of the signal are estimated and removed from the weaker signal to enable the other carrier loop to operate with a smaller bandwidth and, hence, a higher loop SNR. In the second scenario, the signal is too weak to be tracked by any single antenna but can be tracked jointly by two or more antennas. The combining methods used in the latter case are similar to those employed in FSC when aligning the phases of pure tones (hence, requiring a smaller correlator bandwidth). In either scenario, carrier arraying can be implemented in one of two ways: at baseband or at an intermediate frequency (IF). Both implementations are discussed in the next sections.

1. Baseband Carrier Arraying Scheme. Baseband carrier arraying is illustrated in Fig. 13 where the error

signals at the output of the phase detectors are combined at baseband. This scheme is analyzed in [12] where it is shown that the variance of the phase jitter process in the master PLL is given by

$$\sigma_{c1}^2 = \frac{1}{2\pi j}\oint \left[\frac{H_1(z)}{1+\sum_{i=2}^{L}\gamma_i H_1(z)[1-H_i(z)]}\right]^2 \frac{dz}{z}\frac{N_{01}}{2T_{c1}P_{c1}}$$

$$+\sum_{i=2}^{L}\gamma_i^2\frac{1}{2\pi j}\oint \left[\frac{H_1(z)[1-H_i(z)]}{1+\sum_{i=2}^{L}\gamma_i H_1(z)[1-H_i(z)]}\right]^2 \frac{dz}{z}\frac{N_{0i}}{2T_{ci}P_{ci}} \tag{76}$$

where $H_i(z)$ is the closed-loop transfer function of the ith loop, T_{ci} is the loop update time, and γ_i is as defined in Eq. (32). The above integral is difficult to evaluate in general. However, when $B_{ci} \ll B_{c1}$ for $i = 2, \ldots, L$, which is the preferred mode of operation, the above integral can be approximated by

$$\sigma_{c1}^2 \approx \frac{B_{c1}\sum_{i=1}^{L}\beta_i^2 N_{0i}}{P_{c1}\Gamma^2} \tag{77}$$

which assumes ideal performance. In this case, the master loop SNR becomes

$$\rho_{c1} = \frac{P_{c1}}{B_{c1}N_{01}}\Gamma \tag{78}$$

assuming identical noise spectral densities. The actual variance will typically be larger and requires the evaluation of Eq. (76), which depends on the actual loop filters implemented.

2. IF Carrier Arraying Scheme. One form of IF carrier arraying is depicted in Fig. 14 and is conceptually the same as full spectrum combining. In this case, the total power, P_i, is substituted for by the carrier power, P_{ci}. So, all equations and results derived in Section III.C regarding the combining loss can be automatically applied to the IF carrier arraying scheme. Phase estimation in this case can be performed by downconverting the received IFs to baseband using a precomputed model of the received Doppler and Doppler rate. The correlation can be computed at baseband using "very small" bandwidths B and, hence, requiring "short" integration times T. From Eq. (52), the variance of the ith carrier correlator is

$$\sigma_{ci}^2 = B(N_{01}P_{ci} + N_{0i}P_{c1}) + N_{01}N_{0i}B^2$$

$$\approx N_{01}N_{0i}B^2 \tag{79}$$

while the correlator's SNR is

$$SNR_{c,\,i1} \simeq \frac{P_{c1}}{N_{01}}\frac{P_{ci}}{N_{0i}}\frac{2T}{B} \tag{80}$$

Note that for IF carrier arraying, the bandwidth B is much narrower than for full spectrum combining since the data spectrum is not employed.

The signal combiner performs the weighted sum of carrier signals $\mathbf{c}_i(t)$, giving the complex combined carrier signal

$$\mathbf{c}(t) = \sum_{i=1}^{L}\beta_i\left[\sqrt{P_{ci}}e^{j[\omega_I t+\theta_1(t)+\Delta\phi_{c,i}(t)]}\right.$$

$$\left. + \mathbf{n}_i(t)e^{j[\omega_I t+\theta_1(t)+\Delta\phi_{c,i}(t)]}\right] \tag{81}$$

Following Eqs. (65) through (68), the average carrier power and the variance of the combined complex carrier signal $\mathbf{c}(t)$ are, respectively,

$$P_{\mathbf{c}} = \sum_{i=1}^{L}\beta_i^2 P_{ci} + \sum_{i=1}^{L}\sum_{\substack{k=1\\ i\neq k}}^{L}\beta_i\beta_k\sqrt{P_{ci}P_{ck}}\,\mathbf{C}_{c,\,ik}$$

$$= P_{c1}\left(\sum_{i=1}^{L}\gamma_i^2 + \sum\sum_{\substack{i,j\\ i\neq j}}\gamma_i\gamma_j C_{c,\,ij}\right) \tag{82}$$

and

$$\sigma_{\mathbf{c}}^2 = 2B\sum_{i=1}^{L}\beta_i^2 N_{0i} \tag{83}$$

where

$$C_{c,\,ij} = \mathcal{E}\left\{e^{j[\Delta\phi_{c,i1}(t_k)-\Delta\phi_{c,j1}(t_k)]}\right\}$$

$$= \begin{cases} e^{-\frac{1}{2}\left[\sigma^2_{\Delta\phi_{c,i1}}+\sigma^2_{\Delta\phi_{c,j1}}\right]} & i\neq j,\ \sigma^2_{\Delta\phi_{c,i1}} \equiv 0 \\ 1 & i = j \end{cases} \tag{84}$$

and

$$\sigma^2_{\Delta\phi_{c,ij}} = \frac{1}{SNR_{cij}} \tag{85}$$

To illustrate the results with a simple example, let $P_{ci} = P_{c1}$, $N_{0i} = N_{01}$, and $\beta_i = 1$ for all antennas. Then the signal and noise powers of the real process at the output of the carrier combiner become, respectively,

$$P_c = P_{c1}\left[L + 2(L-1)e^{-(\sigma^2_{\Delta\phi,\,c})/2} + (L-2)(L-1)e^{-\sigma^2_{\Delta\phi,\,c}}\right]$$

and

$$\sigma^2_{\Delta\phi,\,c} = BLN_{01} \tag{86}$$

resulting in a correlator SNR

$$SNR_c = \frac{P_c}{\sigma^2_{\Delta\phi,\,c}} = \frac{P_{c1}\left[L + 2(L-1)e^{-(\sigma^2_{\Delta\phi,\,c})/2} + (L-2)(L-1)e^{-\sigma^2_{\Delta\phi,\,c}}\right]}{LN_{01}B} \tag{87}$$

In an ideal scenario, $\sigma^2_{\Delta\phi,\,c} \to 0$ and

$$SNR_{c,\,ideal} = \frac{P_{c1}L}{N_{01}B} \tag{88}$$

The combining degradation in decibels for IF carrier arraying becomes

$$D_{ifc} = 10\log_{10}\left[\frac{L + 2(L-1)e^{-(\sigma^2_{\Delta\phi,\,c})/2} + (L-2)(L-1)e^{-\sigma^2_{\Delta\phi,\,c}}}{L^2}\right] \tag{89}$$

E. Arraying Combinations

Besides the individual arraying schemes described in this article, combinations of them can be implemented. In particular, SSC can be enhanced with SA and with CA. Similarly, BC can be enhanced with SA and with CA. FSC uses only one set of receiver, subcarrier, and symbol tracking loops, but, again, the performance of the receiver can be improved with SA. A general symbol SNR degradation function, which is applicable to any arraying scheme, is given in Appendix C, Table C-2.

A comparison of all schemes and arraying combinations is depicted in Figs. 15(a) and (b), where the degradations of BC, SSC, FSC, SSC/SA/CA, FSC/SA, BC/SA/CA, SSC/CA, SSC/SA, BC/SA, and BC/CA are all computed versus P_T/N_0 for a fixed $\Delta = 65.9$ deg. These curves were computed assuming $B_T = 0.1$ mHz and $B_n = 135$ kHz for the RTC, $T/B = 0.0008$ sec^2 for FSC, $T/B = 0.075$ sec^2 for CA (assumed at IF), and a symbol rate of 34 symbols per sec (sps). From Fig. 15(a), it seems that the three schemes with the least degradation at 20 dB-Hz are FSC/SA, BC/CA/SA, and SSC/SA/CA. Most schemes seem to maintain an 8-dB minimum carrier loop SNR for P_T/N_0 as low as 20 dB-Hz, except for SSC and BC which loose lock at roughly 24 dB-Hz and BC/CA, and SSC/CA which requires a $P_T/N_0 \geq 21$ dB-Hz. Recall that the delay adjustment in FSC and FSC/SA was assumed perfect resulting in no degradation. More realistically, a 0.05-dB or a 0.1-dB degradation should be added and, hence, FSC/SA and BC/SA/CA seem to provide identical degradations.

For this particular case, FSC requires 216 sec of integration length (for $T/B = 0.0008$ sec^2 and $B = 2 \times 135$ kHz), a rather unrealistic parameter. For a shorter integration time (on the order of a few seconds), the correlator SNR degrades significantly and the differential phase cannot be estimated. The bandwidth B can be reduced to pass only the first harmonic of the subcarrier, but that still results in unrealistic integration times. The signal can be passed through a "matched filter," which passes the subcarrier harmonics and the data modulation, but rejects the spectrum between the harmonics. The effective bandwidth of such a filter would be on the order of the symbol rate and, hence, results in shorter integration times as long as the subcarrier frequency is a "large" multiple of the symbol rate ($m \gg 1$). The drawback of such a filter is that it is too specific to the signal of interest and needs to be modified for each mission. Moreover, it might

require frequency tuning to center the signal in the band of interest. Another technique to reduce the bandwidth is to only correlate the residual carrier components in order to further shorten the integration time. This is precisely the technique employed in carrier arraying, when implemented at IF. It should be pointed out that even though the phase is adjusted at IF, it can and should be estimated at baseband by mixing the received IF from each antenna with a Doppler and a Doppler rate predict of the signal. The outputs of the mixers consist of a tone with a very low frequency component which requires a "very small" bandwidth B prior to the correlation. With $T/B = 0.075$ sec^2 and $T = 3$ sec, $B = 2 \times 20$ Hz, which requires the frequency predicts to be correct to within ± 20 Hz. Even if the error is larger than ± 20 Hz, a fast Fourier transform can be used to reduce the frequency error at the output of the mixers such that it lies well within $B/2$ Hz.

As seen from the above example, FSC/SA and BC/SA/CA provide the least degradation and, hence, the "best" performance overall, but BC/CA/SA accomplishes that with reasonable integration times. SA is enhancing the performance in both cases because the carrier component is so weak due to the high modulation index and relatively low received power. For signals with stronger carriers, FSC and FSC/SA would provide similar degradations for all practical purposes, as would BC/CA and BC/SA/CA. It is worth noting at this point that FSC, as presented in this article, compensated for the signal delays up front and then adjusted for the phases. This is the classical arraying performed in radiometry. However in BC/CA, CA is first employed to lock on the signal (hence, a phase adjustment) and later, delay compensation is performed in the BBA to coherently add the data. The latter, which is equivalent in performance to FSC (but with shorter integration times), seems to be favored more by communication engineers whereas FSC seems to be favored more by astrophysicists. The major difference between FSC and BC/CA is the integration length required to estimate the differential phase. BC/CA offers a significant advantage by requiring much shorter integration times for spacecraft with very weak signals and a large subcarrier-to-data-rate ratio.

In either FSC or BC/CA, atmospheric effects can be significant, especially at higher frequencies and in the presence of thunderstorms. Figure 16 depicts the relative phase along baseline "1–3" in the VLA on a clear night and in the presence of thunderstorms. In the latter case, the integration time T needs to be short to track the phase variation. The resulting combining degradation can be 0.2 dB or even more depending on the scenario.

IV. Numerical Examples

The results derived in this article were applied to several existing deep-space missions in order to illustrate the differences in combined symbol SNR performance. The missions considered were Pioneer 10, Voyager 2, and Magellan, reflecting weak, medium, and strong signals, respectively, in the DSN. As expected, the weaker the signal, the harder it is to array the antennas.

A. Pioneer 10

The signal received from Pioneer 10 represents the weakest signal in the DSN. It is an S-band signal with the following characteristics as of May 1990:

(1) symbol rate $R_s = 32$ sps

(2) subcarrier frequency $f_{sc} = 32768$ Hz

(3) modulation index $\Delta = 65.9$ deg

The receiver is assumed to operate with the following parameters:

(1) $B_c = 1.5$ Hz for the carrier bandwidth (Block IV Receiver)

(2) $B_{sc} = B_{sy} = 0.1$ Hz for subcarrier and symbol tracking loops

(3) $B_\tau = 0.1$ mHz and $B_n = 135$ kHz for the RTC

(4) $T/B = 0.075$ sec^2, $B = 2 \times 20$ Hz, and $T = 3$ sec for carrier arraying

(5) $T/B = 0.0008$ sec^2 for FSC with regular IF filters ($B = 2 \times 135$ kHz and $T = 216$ sec)

(6) $T/B = 0.0008$ sec^2 for FSC with "matched" filter [$B = 5 \times (2 \times 50)$ Hz and $T = 0.4$ sec], where the factor 5 accounts for the first five odd subharmonics of the square-wave subcarrier.

Two array configurations are considered: a 70-m and 34-m STD antenna array, which can provide 0.68-dB gain (over the 70-m antenna) in the ideal case, and an array of two 70-m antennas (providing an ideal 3-dB gain). The degradations for both arrays are shown in Tables 1 and 2, respectively. The 20–dB-Hz signal represents the approximate level at the master antenna, in this case, the 70-m antenna.

In the first array (the 70-m plus STD 34-m antennas), BC and SSC cannot operate due to the inability of the STD 34-m antenna to maintain carrier lock. However, BC/SA and SSC/SA can operate with an 8-dB loop SNR, which is the minimum required to avoid cycle slipping. FSC/SA

achieves the highest loop SNR at 18.2 dB, followed by BC/SA/CA and SSC/SA/CA at 17.7 dB, and followed finally by BC/SA, SSC/SA, and FSC at 11 dB. The smallest degradations are obtained with FSC/SA and BC/SA/CA at about 0.53 dB. Note that the combining loss of FSC at 0.19 dB can be reduced by integrating over longer periods. In the array of two 70-m antennas, all schemes maintain lock as expected with the smallest degradation achieved by FSC/SA at 0.34 dB and the largest achieved by BC at 0.81 dB. FSC/SA seems to be the best arraying scheme for Pioneer 10 and the sideband aiding is essential in reducing the degradation. However, recall that the long integration time required in FSC/SA renders the scheme impractical; hence, BC/CA/SA is really the best scheme for Pioneer 10.

B. Voyager 2

Unlike Pioneer 10, Voyager 2 can be tracked by all 34-m antennas in the DSN. It represents a medium signal in both received power and data rate. The X-band signal processes the following characteristics:

(1) symbol rate $R_s = 43.2$ sps

(2) subcarrier frequency $f_{sc} = 360$ kHz

(3) modulation index $\Delta = 77$ deg

The receivers are assumed to operate with the following parameters:

(1) $B_c = 10$ Hz for the carrier bandwidth

(2) $B_{sc} = B_{sy} = 1.0$ Hz for subcarrier and symbol tracking loops

(3) $B_\tau = 1$ mHz and $B_n = 3.2$ MHz for the RTC

(4) $T/B = 0.075$ sec^2 for carrier arraying

(5) $T/B = 2.0 \times 10^{-7}$ sec^2, $B = 3.2$ MHz, and $T = 1.3$ sec for FSC

Table 3 provides the degradations for all arraying schemes for a three-element array of one HEF 34-m and two STD 34-m antennas. This array can provide an ideal 3-dB gain over the HEF 34-m master antenna, with $P_T/N_0 = 39$ dB-Hz. The second array, whose performance is shown in Table 4, also consists of three elements: one 70-m, one STD 34-m, and one HEF 34-m antenna. The master in this case is the 70-m antenna with $P_T/N_0 = 45$ dB-Hz. This array can provide a maximum gain of 1.43 dB. BC/SA, BC/CA, and BC/SA/CA can provide the smallest degradations if the combining loss is maintained below 0.01 dB. On the other hand, FSC/SA provides a better performance for a more realistic 0.07-dB IF degradation. For all practical purposes, both FSC and BC/CA perform equally with realistic integration times.

C. Magellan

The highest data rate signal is transmitted by Magellan at X-band with

(1) symbol rate $R_s = 537.6$ ksps

(2) subcarrier frequency $f_{sc} = 960$ kHz

(3) modulation index $\Delta = 78$ deg

Tables 5 and 6 provide the degradations for an array of one HEF 34-m and one STD 34-m antenna (providing a 1.76-dB ideal gain over the HEF 34-m master antenna) and another array of one 70-m, one HEF 34-m, and one STD 34-m antenna (providing a 1.43-dB ideal gain over the 70-m master antenna). The receivers are assumed to operate with

(1) $B_c = 30$ Hz for carrier bandwidth

(2) $B_{sc} = B_{sy} = 3.0$ Hz for subcarrier and symbol tracking loops

(3) $B_\tau = 10$ mHz and $B_n = 4.5$ MHz for the RTC

(4) $T/B = 0.075$ sec^2 for carrier arraying

(5) $T/B = 1.0 \times 10^{-10}$ sec^2 for FSC

In this case, all combining methods provide near-optimum performances for both arrays.

V. Conclusions

Four different arraying schemes have been investigated and these include symbol stream combining, baseband combining, carrier arraying, and full spectrum combining. For DSN applications where telemetry signal reception is the primary concern, BC/CA and BC/CA/SA provide the best arraying schemes for very weak signals with large subcarrier-frequency-to-data-rate ratios. FSC and FSC/SA are not well suited for these scenarios, but can be made so by employing "matched filters" at the cost of additional complexity. For moderate to high signal levels, FSC and BC/CA are both well suited and provide comparable performances.

Acknowledgments

The authors thank D. Rogstad for his numerous discussions and J. Ulvestad for providing Fig. 16 on the VLA thunderstorm data. Special thanks to G. Resch for suggesting the idea of the article and to J. Statman for his valuable comments while reviewing this article.

References

[1] J. W. Layland, P. J. Napier, and A. R. Thompson, "A VLA Experiment—Planning for Voyager at Neptune," *TDA Progress Report 42-82,* vol. April–June 1985, Jet Propulsion Laboratory, Pasadena, California, pp. 136–142, August 15, 1985.

[2] J. S. Ulvestad, "Phasing the Antennas of the Very Large Array for Reception of Telemetry from Voyager 2 at Neptune Encounter," *TDA Progress Report 42-94,* vol. April–June 1988, Jet Propulsion Laboratory, Pasadena, California, pp. 257–273, August 15, 1988.

[3] J. Yuen, *Deep Space Telecommunications Systems Engineering,* New York: Plenum Press, 1982.

[4] S. Hinedi, "A Functional Description of the Advanced Receiver," *TDA Progress Report 42-100,* vol. October–December 1989, Jet Propulsion Laboratory, Pasadena, California, February 15, 1990, pp. 131–149.

[5] R. Sfeir, S. Aguirre, and W. Hurd, "Coherent Digital Demodulation of a Residual Signal Using IF Sampling," *TDA Progress Report 42-78,* vol. April–June 1984, Jet Propulsion Laboratory, Pasadena, California, pp. 135–142, August 15, 1984.

[6] W. Lindsey and M. Simon, *Telecommunication Systems Engineering,* New Jersey: Prentice-Hall, 1973.

[7] W. Hurd and S. Aguirre, "A Method to Dramatically Improve Subcarrier Tracking," *TDA Progress Report 42-86,* vol. April–June 1986, Jet Propulsion Laboratory, Pasadena, California, pp. 103–110, August 15, 1986.

[8] W. J. Hurd, J. Rabkin, M. D. Russel, B. Siev, H. W. Cooper, T. O. Anderson, and P. U. Winter, "Antenna Arraying of Voyager Telemetry Signals by Symbol Stream Combining," *TDA Progress Report 42-86,* vol. April–June 1986, Jet Propulsion Laboratory, Pasadena, California, pp. 131–142, August 15, 1986.

[9] D. Divsalar, "Symbol Stream Combining Versus Baseband Combining for Telemetry Arraying," *TDA Progress Report 42-74,* vol. April–June 1983, Jet Propulsion Laboratory, Pasadena, California, pp. 13–28, August 15, 1983.

[10] M. K. Simon and A. Mileant, *Performance Analysis of the DSN Baseband Assembly Real-Time Combiner,* JPL Publication 84-94, Revision 1, Jet Propulsion Laboratory, Pasadena, California, May 1, 1985.

[11] R. M. Hjellming, ed., *An Introduction to the NRAO Very Large Array,* National Radio Astronomy Observatory, Socorro, New Mexico, 1980.

[12] D. Divsalar and J. Yuen, "Improved Carrier Tracking Performance with Coupled Phase-Locked Loops," *TDA Progress Report 42-66,* vol. April–June 1981, Jet Propulsion Laboratory, Pasadena, California, pp. 148–171, August 15, 1981.

Table 1. Pioneer 10, one 70-m and one STD 34-m antenna array

Arraying scheme	P_T/N_0, dB-Hz	Total degradation, dB	Carrier degradation, dB	Subcarrier degradation, dB	Symbol degradation, dB	RTC or IF degradation, dB
BC	20.00	no	carrier	lock	—	—
BC+SA	20.00	−0.614	−0.17	−0.25	−0.07	−0.12
BC+CA	20.00	−0.792	−0.34	−0.26	−0.08	−0.12
BC+SA+CA	20.00	−0.526	−0.07	−0.26	−0.08	−0.12
SSC	20.00	no	carrier	lock	—	—
SSC+SA	20.00	−0.670	−0.17	−0.39	−0.11	0.00
SSC+CA	20.00	−0.849	−0.34	−0.40	−0.11	0.00
SSC+SA+CA	20.00	−0.583	−0.07	−0.40	−0.11	0.00
FSC	20.00	−0.874	−0.35	−0.26	−0.08	−0.19
FSC+SA	20.00	−0.593	−0.07	−0.26	−0.08	−0.19
FSC (matched filter)	20.00	−0.874	−0.35	−0.26	−0.08	−0.19
FSC+SA (matched filter)	20.00	−0.593	−0.07	−0.26	−0.08	−0.19

Table 2. Pioneer 10, two 70-m antenna arrays

Arraying scheme	P_T/N_0, dB-Hz	Total degradation, dB	Carrier degradation, dB	Subcarrier degradation, dB	Symbol degradation, dB	RTC or IF degradation, dB
BC	20.00	−0.812	−0.40	−0.19	−0.06	−0.17
BC+SA	20.00	−0.487	−0.08	−0.19	−0.06	−0.17
BC+CA	20.00	−0.608	−0.20	−0.19	−0.06	−0.17
BC+SA+CA	20.00	−0.475	−0.06	−0.19	−0.06	−0.17
SSC	20.00	−0.768	−0.40	−0.29	−0.08	0.00
SSC+SA	20.00	−0.444	−0.08	−0.29	−0.08	0.00
SSC+CA	20.00	−0.565	−0.20	−0.29	−0.08	0.00
SSC+SA+CA	20.00	−0.432	−0.06	−0.29	−0.08	0.00
FSC	20.00	−0.509	−0.20	−0.19	−0.06	−0.07
FSC+SA	20.00	−0.347	−0.04	−0.19	−0.06	−0.07
FSC (matched filter)	20.00	−0.509	−0.20	−0.19	−0.06	−0.07
FSC+SA (matched filter)	20.00	−0.347	−0.04	−0.19	−0.06	−0.07

Table 3. Voyager 2, one master HEF 34-m and two STD 34-m antenna arrays

Arraying scheme	P_T/N_0, dB-Hz	Total degradation, dB	Carrier degradation, dB	Subcarrier degradation, dB	Symbol degradation, dB	RTC or IF degradation, dB
BC	39.00	−0.346	−0.16	−0.11	−0.03	−0.04
BC+SA	39.00	−0.219	−0.04	−0.11	−0.03	−0.04
BC+CA	39.00	−0.236	−0.05	−0.11	−0.03	−0.04
BC+SA+CA	39.00	−0.197	−0.02	−0.11	−0.03	−0.04
SSC	39.00	−0.548	−0.16	−0.31	−0.08	0.00
SSC+SA	39.00	−0.422	−0.04	−0.31	−0.08	0.00
SSC+CA	39.00	−0.439	−0.05	−0.31	−0.08	0.00
SSC+SA+CA	39.00	−0.400	−0.02	−0.31	−0.08	0.00
FSC	39.00	−0.284	−0.06	−0.11	−0.03	−0.09
FSC+SA	39.00	−0.235	−0.01	−0.11	−0.03	−0.09

Table 4. Voyager 2, one 70-m, one STD 34-m, and one HEF 34-m antenna array

Arraying scheme	P_T/N_0, dB-Hz	Total degradation, dB	Carrier degradation, dB	Subcarrier degradation, dB	Symbol degradation, dB	RTC or IF degradation, dB
BC	45.00	−0.130	−0.06	−0.05	−0.01	−0.01
BC+SA	45.00	−0.084	−0.01	−0.05	−0.01	−0.01
BC+CA	45.00	−0.091	−0.02	−0.05	−0.01	−0.01
BC+SA+CA	45.00	−0.077	−0.01	−0.05	−0.01	−0.01
SSC	45.00	−0.208	−0.06	−0.12	−0.03	0.00
SSC+SA	45.00	−0.163	−0.01	−0.12	−0.03	0.00
SSC+CA	45.00	−0.170	−0.02	−0.12	−0.03	0.00
SSC+SA+CA	45.00	−0.156	−0.01	−0.12	−0.03	0.00
FSC	45.00	−0.148	−0.02	−0.05	−0.01	−0.07
FSC+SA	45.00	−0.134	−0.01	−0.05	−0.01	−0.07

Table 5. Magellan, one master HEF 34-m and one STD 34-m antenna array

Arraying scheme	P_T/N_0, dB-Hz	Total degradation, dB	Carrier degradation, dB	Subcarrier degradation, dB	Symbol degradation, dB	RTC or IF degradation, dB
BC	59.00	−0.022	−0.01	−0.01	0.00	0.00
BC+SA	59.00	−0.022	−0.01	−0.01	0.00	0.00
BC+CA	59.00	−0.022	−0.01	−0.01	0.00	0.00
BC+SA+CA	59.00	−0.022	−0.01	−0.01	0.00	0.00
SSC	59.00	−0.027	−0.01	−0.02	0.00	0.00
SSC+SA	59.00	−0.027	−0.01	−0.02	0.00	0.00
SSC+CA	59.00	−0.027	−0.01	−0.02	0.00	0.00
SSC+SA+CA	59.00	−0.027	−0.01	−0.02	0.00	0.00
FSC	59.00	−0.036	−0.01	−0.01	0.00	−0.02
FSC+SA	59.00	−0.036	−0.01	−0.01	0.00	−0.02

Table 6. Magellan, one 70-m, one HEF 34-m, and one STD 34-m antenna array

Arraying scheme	P_T/N_0, dB-Hz	Total degradation, dB	Carrier degradation, dB	Subcarrier degradation, dB	Symbol degradation, dB	RTC or IF degradation, dB
BC	65.00	−0.015	−0.01	−0.01	0.00	0.00
BC+SA	65.00	−0.015	−0.01	−0.01	0.00	0.00
BC+CA	65.00	−0.015	−0.01	−0.01	0.00	0.00
BC+SA+CA	65.00	−0.015	−0.01	−0.01	0.00	0.00
SSC	65.00	−0.021	−0.01	−0.01	0.00	0.00
SSC+SA	65.00	−0.021	−0.01	−0.01	0.00	0.00
SSC+CA	65.00	−0.021	−0.01	−0.01	0.00	0.00
SSC+SA+CA	65.00	−0.021	−0.01	−0.01	0.00	0.00
FSC	65.00	−0.031	−0.01	−0.01	0.00	−0.02
FSC+SA	65.00	−0.031	−0.01	−0.01	0.00	−0.02

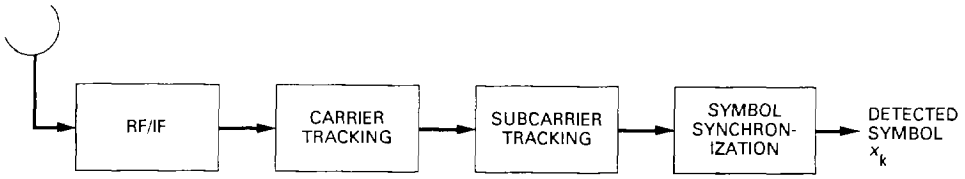

Fig. 1. A general coherent receiver model.

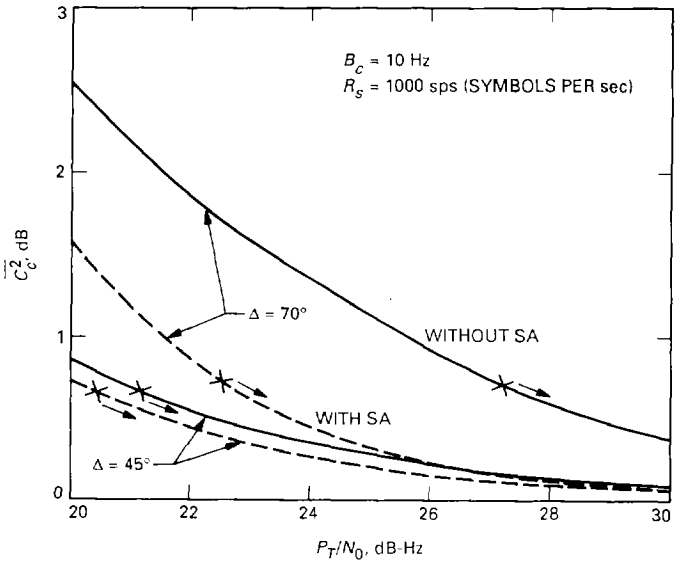

Fig. 2. Symbol SNR degradation due to imperfect carrier reference.

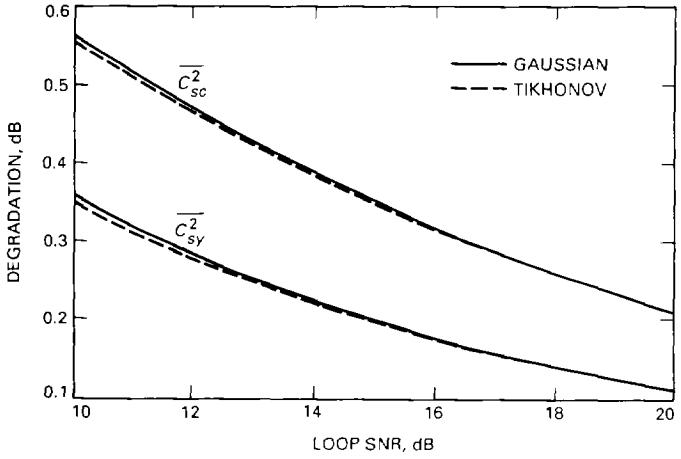

Fig. 3. Symbol SNR degradation in the presence of subcarrier and symbol phase jitter.

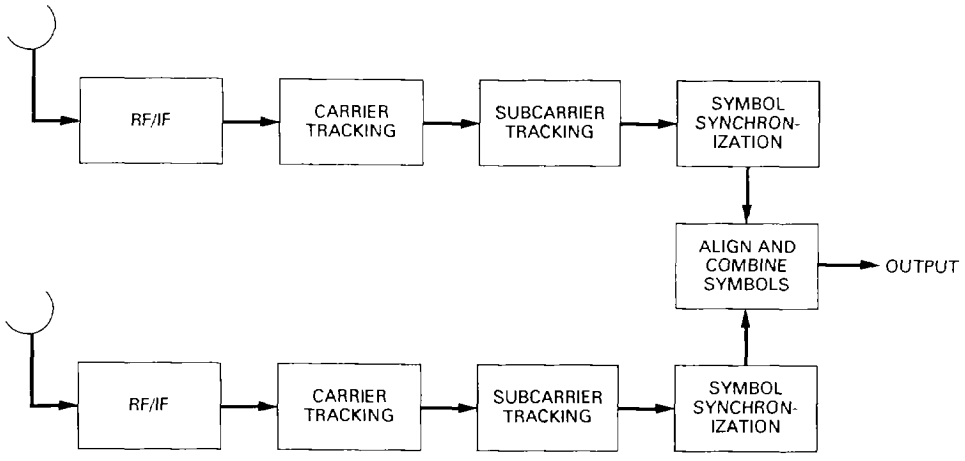

Fig. 4. Symbol stream combining.

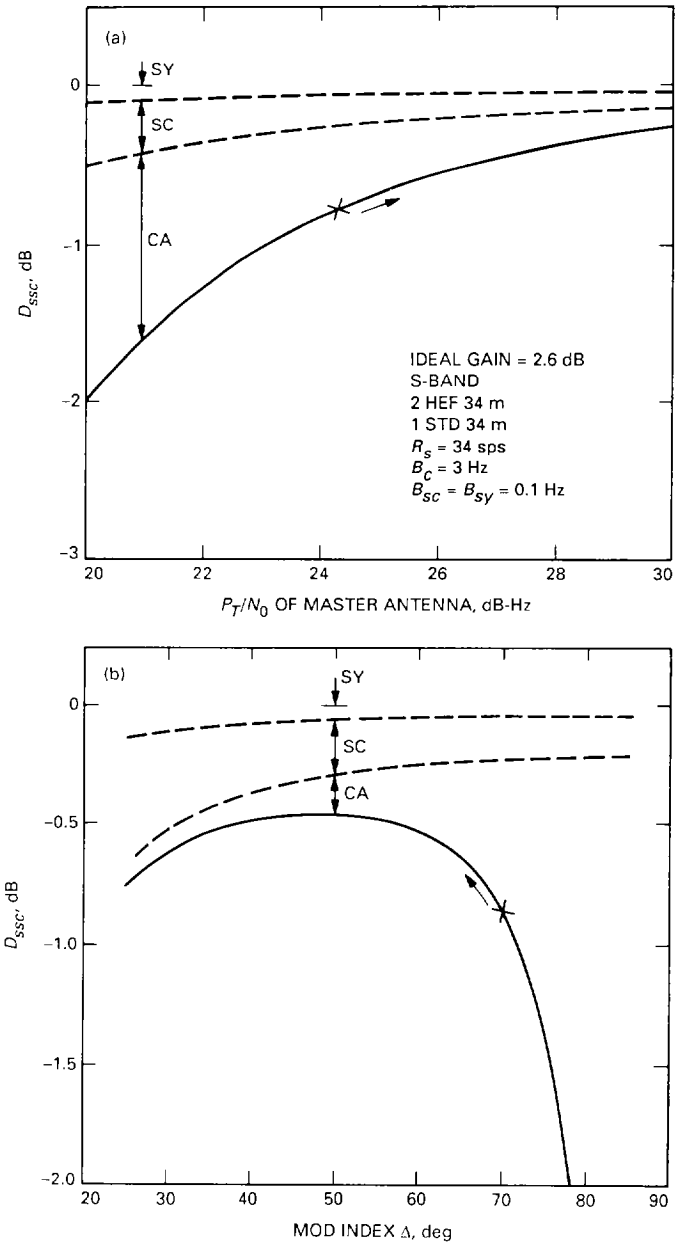

Fig. 5. The D_{ssc} versus: (a) P_T/N_0 for $\Delta = 65.9$ deg, and (b) Δ for $P_T/N_0 = 25$ dB-Hz.

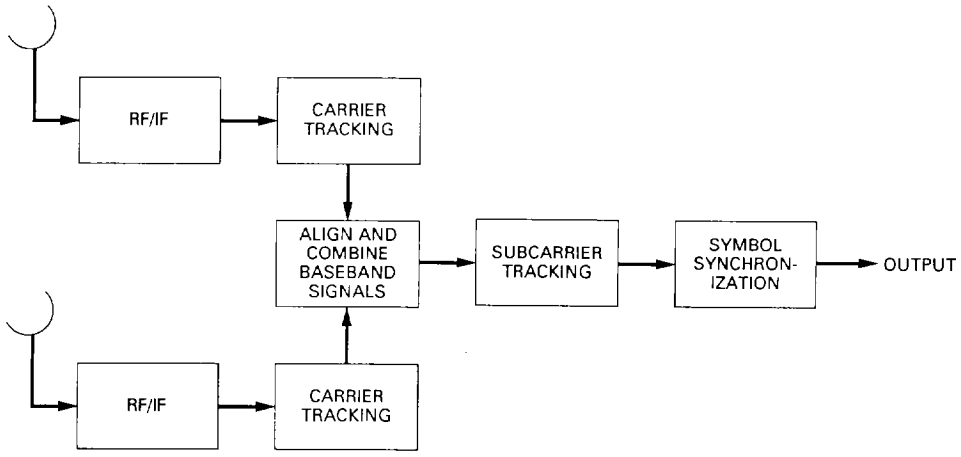

Fig. 6. Baseband combining.

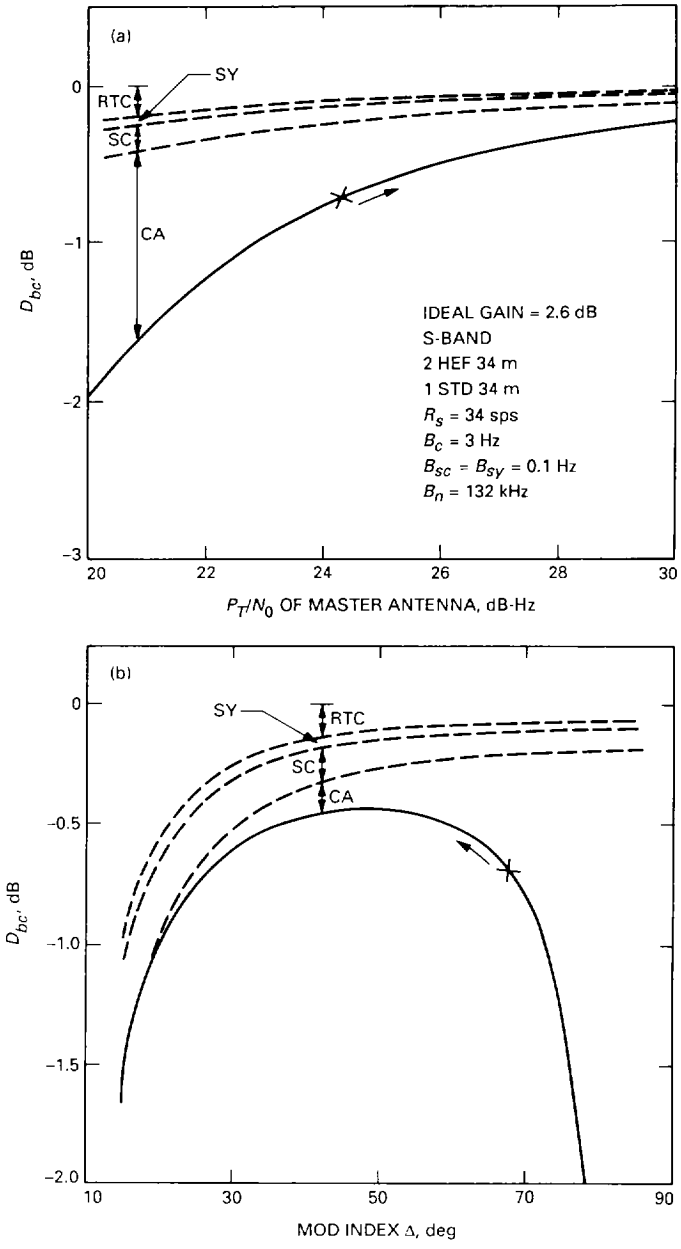

Fig. 7. The D_{bc} versus: (a) P_T/N_0 for $\Delta = 65.9$ deg, and (b) Δ for $P_T/N_0 = 25$ dB-Hz.

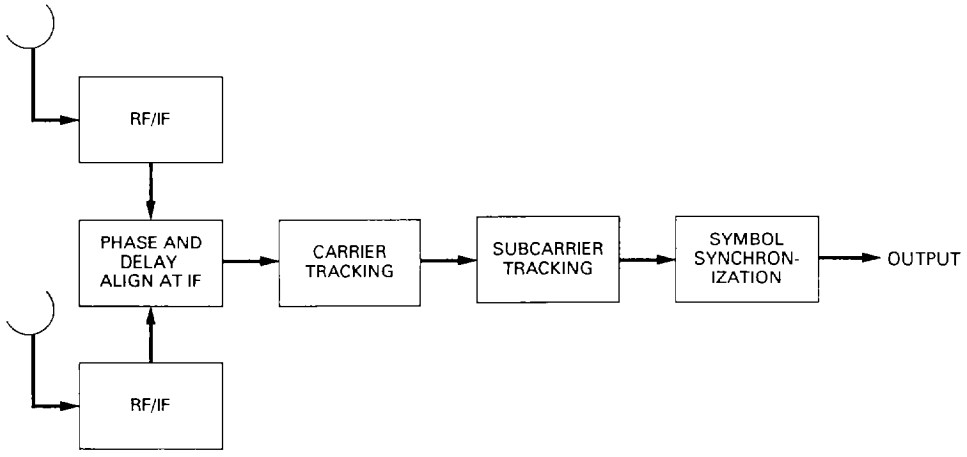

Fig. 8. Full spectrum combining.

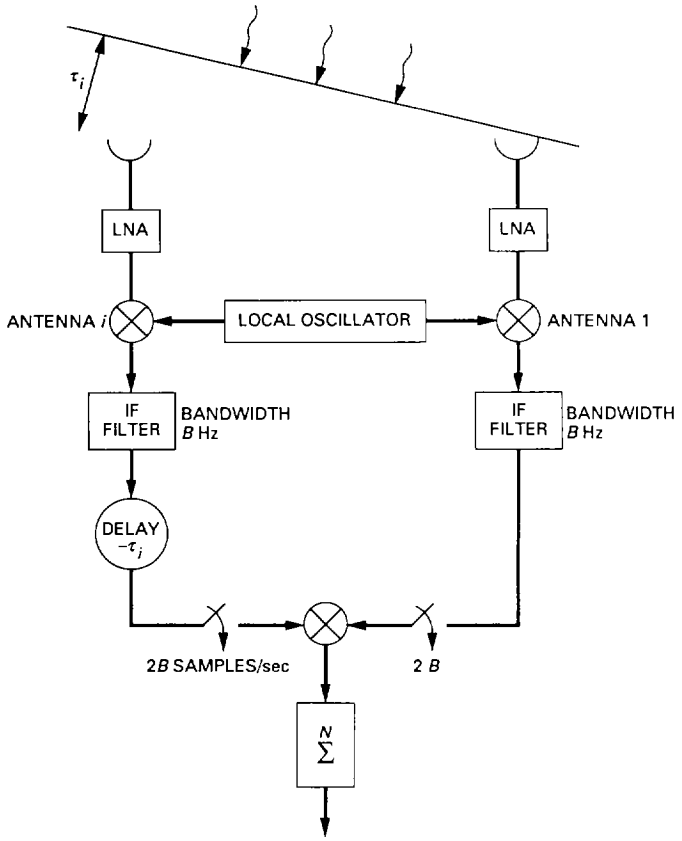

Fig. 9. An interferometric antenna pair.

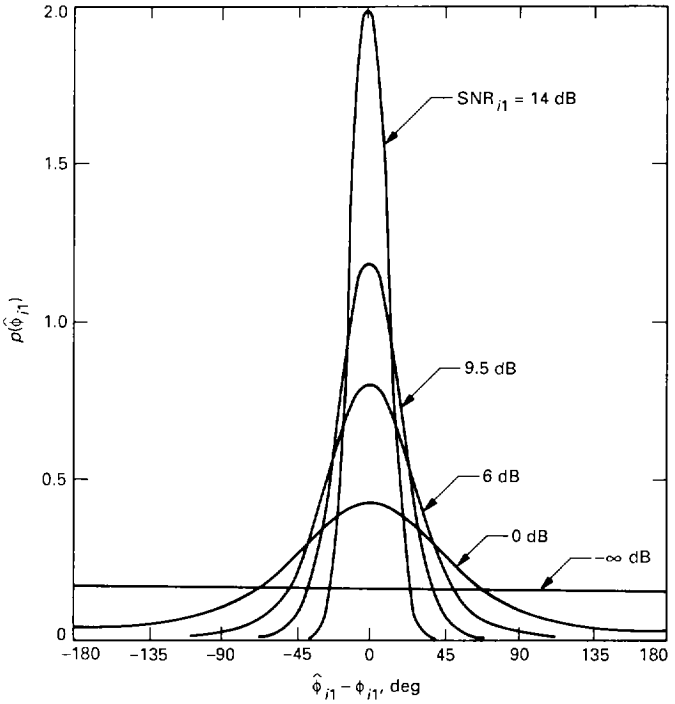

Fig. 10. The probability distribution of measured phase as a function of $\hat{\phi} - \phi$ for a number of signal-to-noise ratios.

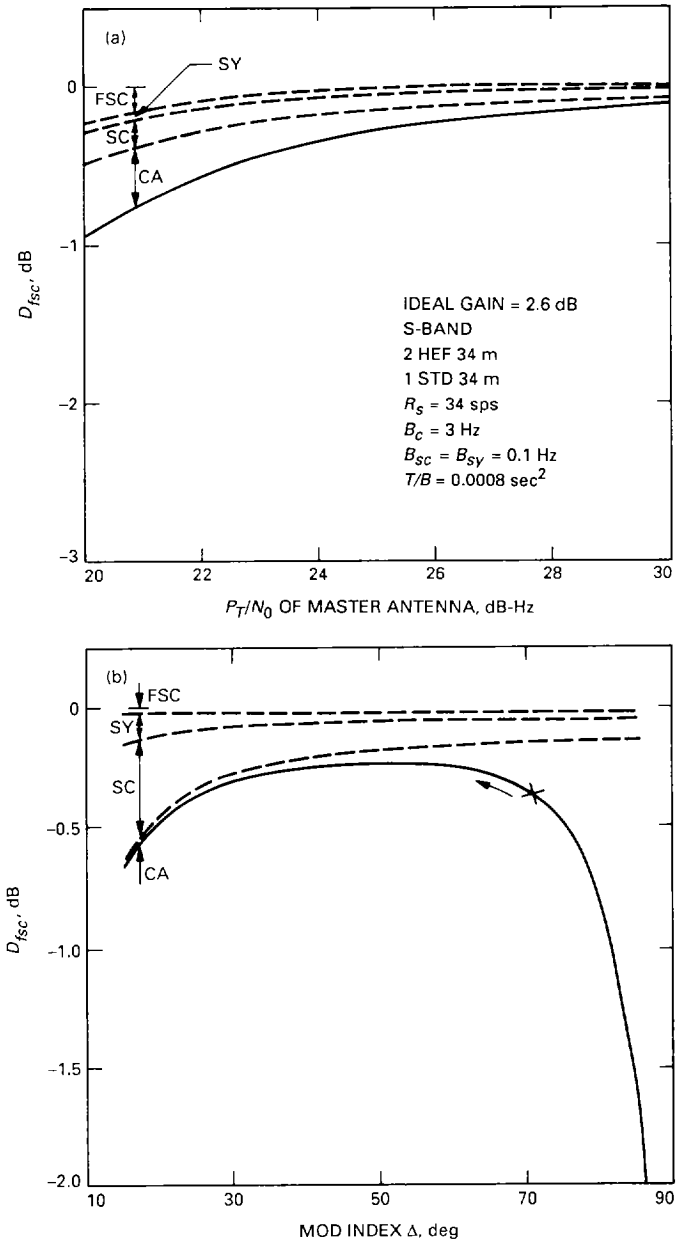

Fig. 11. The D_{fsc} versus: (a) P_T/N_0 for $\Delta = 65.9$ deg, and (b) Δ for $P_T/N_0 = 25$ dB-Hz.

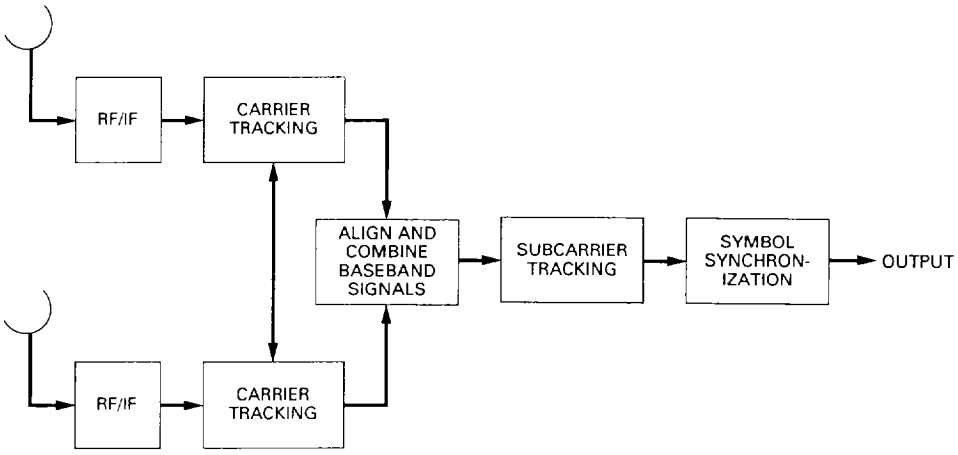

Fig. 12. Carrier arraying with baseband combining (CA/BC).

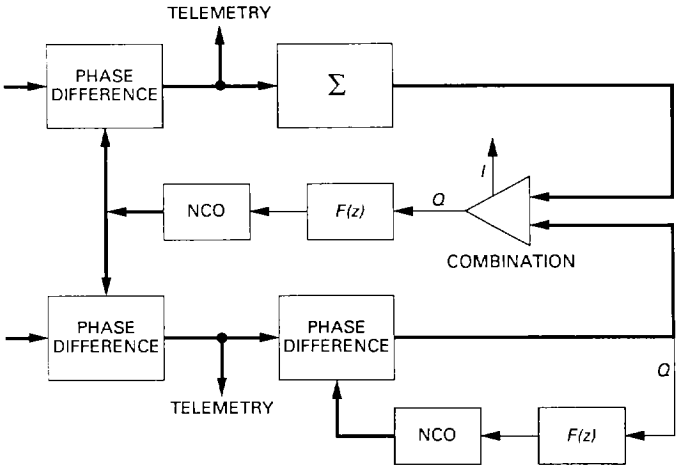

Fig. 13. A baseband implementation of carrier arraying.

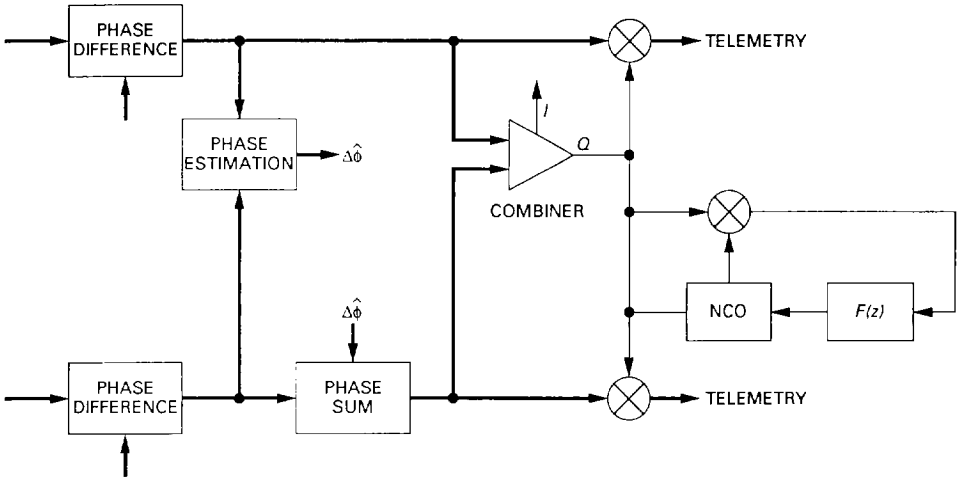

Fig. 14. An IF implementation of carrier arraying.

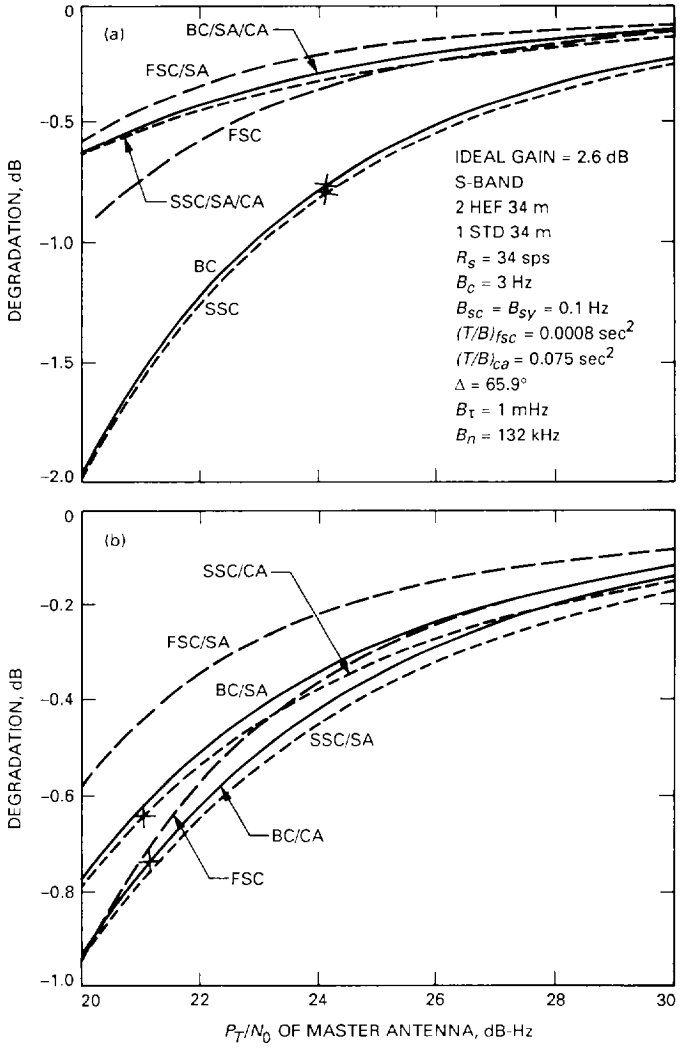

Fig. 15. Comparison of SSC, FSC, and FSC/SA with: (a) BC, SSC/SA/CA, and BC/SA/CA, and (b) BC/CA, BC/SA, and SSC/CA.

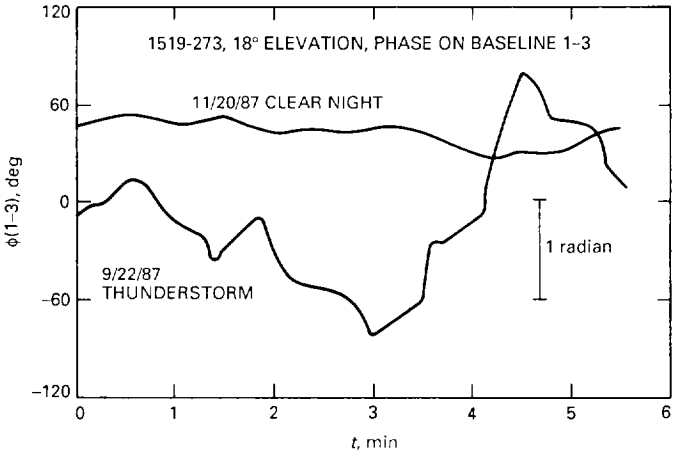

Fig. 16. Very Large Array thunderstorm data at 8.4 GHz.

Appendix A

Gamma Factors for DSN Antennas

Table A-1 summarizes the γ_i factors,[1] defined by Eq. (23), for several DSN antennas at both S-band (2.2 to 2.3 GHz) and X-band (8.4 to 8.5 GHz). Conceptually, these gamma factors represent the antenna gain/noise temperature ratios normalized by the gain/noise temperature of the largest antenna. Here HEF denotes high-efficiency antenna and STD a standard antenna.

The numbers presented below should be used in a relative sense, not in an absolute sense. For example, for a three-element array consisting of one HEF 34-m antenna and two STD 34-m antennas at S-band, the master antenna (in this case, the HEF 34 m) will have $\gamma_1 = 1$ and the other two antennas would have $\gamma_2 = \gamma_3 = 0.13/0.26 = 0.5$.

[1] *Deep Space Network/Flight Project Interface Design Handbook,* Document 810-5, Rev. D, Vol. I (internal document), Jet Propulsion Laboratory, Pasadena, California, Modules TCI-10, TCI-30, and TLM-10, 1988.

Table A-1. Gamma factors for DSN antennas

Antenna size	Frequency band	γ_i
70 m	S-band	1.00
34 m STD	S-band	0.17
34 m HEF	S-band	0.07
70 m	X-band	1.00
34 m STD	X-band	0.13
34 m HEF	X-band	0.26

Appendix B

Closed-Loop Performance

Typically, one would like to limit the IF combining losses expressed by Eq. (75) to some prespecified maximum value, say D_{max}. Solving Eq. (75) for $\sigma^2_{\Delta\phi\, max}$ yields

$$\sigma^2_{\Delta\phi\, max} < -2 \ln \left[\frac{10^{(D_{max}/10)} L - 1}{L - 1} \right] \tag{B-1}$$

The variance of the phase estimate, $\hat{\phi}_{i1}$, can be reduced by either increasing the correlation time T in Eq. (57) or by tracking the phase error process in a closed-loop fashion. Note that the value of B in Eq. (57) is set by the bandwidth of the telemetry spectrum and cannot be reduced at will.

In the simplest closed-loop implementation of the full spectrum combining scheme, phase-error estimates can be updated using the following difference equation:

$$\hat{\theta}(n) = \hat{\theta}(n-1) + \alpha\phi(n) \tag{B-2}$$

where the value of α can be set between 0.2 and 0.5 and $\hat{\theta}(n)$ is the filtered phase error estimate. The above difference equation gives the following loop transfer function:

$$G(z) = \frac{\hat{\Theta}(z)}{\Phi(z)} = \frac{\alpha}{z-1} \tag{B-3}$$

The variance of the closed-loop phase error process will now be

$$\sigma^2_{i1} = I_1 \sigma^2_{\Delta\phi,\, i1} = I_1 \frac{N_{01} N_{oi} B}{P_1 P_i 2T} \tag{B-4}$$

where

$$I_1 = \frac{1}{2\pi j} \oint |H(z)|^2 \frac{dz}{z} \tag{B-5}$$

and $H(z) = G(z)/[1 + G(z)]$. Using the above $G(z)$ gives

$$I_1 = \frac{\alpha}{2 - \alpha} \tag{B-6}$$

As an example, for $\alpha = 0.2$, $I_1 = 0.11$ and the variance of the phase jitter is reduced by a factor of 10.

Appendix C

Generalization of the Symbol SNR Degradation Function

By comparing the symbol SNR degradation factors that were obtained for different arraying schemes, one arrives at the following general equation of SNR degradation for combinations of arraying schemes:

$$D = 10\log_{10}\left(\overline{C_A^2}\,\frac{\sum_{i=1}^{L}\gamma_i^2\overline{C_{B_i}^2} + \sum\sum_{\substack{i,j\\ i\neq j}}\gamma_i\gamma_j\overline{C_{B_i}}\;\overline{C_{B_j}}}{\Gamma^2}\right) \tag{C-1}$$

where the particular signal reduction factors C_A and C_{Bi} are summarized in Table C-1.

Without SA, the carrier loop SNR is $\rho_{c,r} \triangleq 1/\sigma_{c,r}^2 = P_C/(N_0 B_c)$, while with SA, the loop SNR becomes $\rho_c = \rho_{c,r} + \rho_{c,s}$, where $\rho_{c,s}$ is given in Eq. (10). Note that in BC and FSC, P_D is the combined data power, reduced somewhat by the combining loss.

Table C-1. Comparison of signal reduction factors for different arraying schemes

Item	SSC	SSC+CA	BC	BC+CA	FSC
C_A	1	C_c	$C_{sc}\,C_{sy}$	$C_c\,C_{sc}\,C_{sy}$	$C_c\,C_{sc}\,C_{sy}$
C_{B_i}	$C_{ci}\,C_{sci}\,C_{syi}$	$C_{sci}\,C_{syi}$	$C_{ci}\,C_{\tau i}$	$C_{\tau i}$	C_{IF_i}

Table C-2. Signal reduction factors

Definition	Reduction function	First moment	Second moment	Variance
C_c	$\cos\phi$	$\frac{I_1(\rho_c)}{I_0(\rho_c)}$	$\frac{1}{2}\left[1+\frac{I_2(\rho_c)}{I_0(\rho_c)}\right]$	$\sigma_{c,r}^2 = \frac{N_0 B_c}{P_C}$
C_{sc}	$1-\frac{2}{\pi}\lvert\phi_{sc}\rvert$	$1-\left(\frac{2}{\pi}\right)^{3/2}\sigma_{sc}$	$1-\sqrt{\frac{32}{\pi^3}}\sigma_{sc}+\frac{4}{\pi^2}\sigma_{sc}^2$	$\left(\frac{\pi}{2}\right)^2 \frac{B_{sc}W_{sc}}{R_s\left(\frac{E_s}{N_0}\right)^2}\left(1+\frac{E_s}{N_0}\right)$
C_{sy}	$1-\frac{1}{2\pi}\lvert\phi_{sy}\rvert$	$1-\sqrt{\frac{1}{2\pi}}\frac{\sigma_{sy}}{\pi}$	$1-\sqrt{\frac{2}{\pi}}\frac{\sigma_{sy}}{\pi}+\frac{\sigma_{sy}^2}{4\pi^2}$	$2\pi^2\frac{B_{sy}W_{sy}}{R_s\frac{E_s}{N_0}\Phi^2\sqrt{\frac{E_s}{N_0}}}$
C_τ	$1-4m\lvert\tau_i\rvert$	$1-4m\sqrt{\frac{2}{\pi}}\sigma_{\tau i}$	$1-8m\sqrt{\frac{2}{\pi}}\sigma_{\tau i}+16m^2\sigma_{\tau i}^2$	$\frac{B_{\tau i}}{B_n 32m^2}\left\{\frac{1}{\left[\operatorname{erf}\left(\sqrt{\frac{P_{D1}}{2\sigma_1^2}}\right)\operatorname{erf}\left(\sqrt{\frac{P_{Di}}{2\sigma_i^2}}\right)\right]^2}-1\right\}$
$\mathbf{C}_{IF_i}\mathbf{C}_{IF_j}^*$	$e^{j[\Delta\phi_{i1}(t_k)-\Delta\phi_{j1}(t_k)]}$	$e^{-\frac{1}{2}\left[\sigma^2_{\Delta\phi_{i1}}+\sigma^2_{\Delta\phi_{j1}}\right]}$	—	$\frac{N_{01}N_{0i}B}{P_{c1}P_{ci}2T}$